



**INSTITUTO POTOSINO DE INVESTIGACIÓN
CIENTÍFICA Y TECNOLÓGICA, A.C.**

POSGRADO EN CIENCIAS APLICADAS

**The Density Matrix Renormalization Group
Applied to an electron-Phonon Hamiltonian**

Tesis que presenta

José Manuel Nápoles Duarte

Para obtener el grado de

Maestro en Ciencias Aplicadas

En la opción de

Nanociencias y Nanotecnología

Director de Tesis:

Dr. Aldo Humberto Romero Castro

San Luis Potosí, S.L.P., marzo de 2006

CONSTANCIA DE APROBACIÓN DE LA TESIS

La tesis "**The Density Matrix Renormalization Group Applied To An Electron-Phonon Hamiltonian**" presentada para obtener el Grado de Maestro en Ciencias Aplicadas con opción en Nanociencia y Nanotecnología fue elaborada por **José Manuel Nápoles Duarte** y aprobada el **2 de marzo de 2006** por los suscritos, designados por el colegio de profesores de la División de Materiales Avanzados del Instituto Potosino de Investigación Científica y Tecnológica, A.C.



Dr. Aldo Humberto Romero Castro
Presidente



Dr. Luis Felipe Lastras Martínez
Secretario



Dr. Román López Sandoval
Sinodal



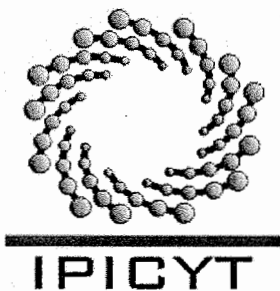
Dr. Haret Codratian Rosu Barbus
Sinodal



CRÉDITOS INSTITUCIONALES

Esta tesis fue elaborada en la División de Materiales Avanzados del Instituto Potosino de Investigación Científica y Tecnológica, A.C., bajo la dirección del doctor Aldo Humberto Romero Castro.

Durante la realización del trabajo el autor recibió una beca académica del Consejo Nacional de Ciencia y Tecnología (No. de registro 182535)



Instituto Potosino de Investigación Científica y Tecnológica, A.C.

Acta de Examen de Grado

COPIA CERTIFICADA

El Secretario Académico del Instituto Potosino de Investigación Científica y Tecnológica, A.C., certifica que en el Acta 016 del Libro Primero de Actas de Exámenes de Grado del Programa de Maestría en Ciencias Aplicadas en la opción de Nanociencias y Nanotecnología está asentado lo siguiente:

En la ciudad de San Luis Potosí a los 2 días del mes de marzo del año 2006, se reunió a las 12:00 horas en las instalaciones del Instituto Potosino de Investigación Científica y Tecnológica, A.C., el Jurado integrado por:

Dr. Aldo Humberto Romero Castro	Presidente	CINVESTAV
Dr. Luis Felipe Lastras Martínez	Secretario	UASLP
Dr. Haret-Codratian Rosu Barbus	Sinodal	IPICYT
Dr. Román López Sandoval	Sinodal	IPICYT

a fin de efectuar el examen, que para obtener el Grado de:

**MAESTRO EN CIENCIAS APLICADAS
EN LA OPCIÓN DE NANOCIENCIAS Y NANOTECNOLOGÍA**

sustentó el C.

José Manuel Nápoles Duarte

sobre la Tesis intitulada:

The Density Matrix Renormalization Group applied to an Electron-Phonon Hamiltonian

que se desarrolló bajo la dirección de

Dr. Aldo Humberto Romero Castro (CINVESTAV)

El Jurado, después de deliberar, determinó

APROBARLO

Dándose por terminado el acto a las 13:40 horas, procediendo a la firma del Acta los integrantes del Jurado. Dando fé el Secretario Académico del Instituto.

A petición del interesado y para los fines que al mismo convengan, se extiende el presente documento en la ciudad de San Luis Potosí, S.L.P., México, a los 2 días del mes marzo de 2006.


L.C.C. Ivonne Lizette Cuevas Velez
Jefa del Departamento de Asuntos Escolares



A mi familia.

AGRADECIMIENTOS

Primero quiero agradecer a mi asesor, el Dr. Aldo H. Romero Castro, por la ayuda que me brindó durante todas las etapas de este trabajo. En este tiempo el me mostró un campo de la física del que yo no tenía mucho conocimiento y además me enseñó la forma en que se desarrolla un proyecto grande como lo es una tesis.

También quiero agradecer al profesor Jereson Silva-Valencia quien vino a enseñarme la construcción de un código DMRG de alto nivel, que de lo contrario me habría tomado mucho tiempo desarrollarlo por mi cuenta. Él también me mostró muchas ideas nuevas de como el DMRG debe implementarse en forma eficiente.

Finalmente agradezco a Joaquín Miranda-Mena con quien pase un tiempo agradable en conversaciones muy instructivas respecto al tema que en esta tesis se trata.

CONTENTS

CONSTANCIA DE APROBACIÓN DE LA TESIS	III
CRÉDITOS INSTITUCIONALES	V
DEDICATORIA	VII
AGRADECIMIENTOS	IX
RESUMEN	XVII
ABSTRACT	XVIII
PREFACE	XIX
1 INTRODUCTION	1
1.1 OUTLINE OF THE THESIS	2
2 QUANTUM MECHANICS: A BRIEF REVIEW	4
2.1 QUANTUM STATES, OPERATORS AND THEIR MAIN PROPERTIES	4
2.2 INVARIANCE IN QUANTUM MECHANICS	6
2.3 MORE ON EIGENVALUE PROBLEMS	7
2.4 COMPOSITE SYSTEMS	8
2.5 SECOND QUANTIZATION	9
2.5.1 BOSONIC OPERATORS	10
2.5.2 FERMIONIC OPERATORS	11

3	THE DMRG METHOD	15
3.1	BASICS ON DMRG	15
3.1.1	DMRG ALGORITHMS	19
3.2	DESCRIPTION OF THE METHOD	26
3.2.1	MANAGEMENT OF HILBERT SPACE	26
4	THE HUBBARD MODEL	31
4.1	SOME ASPECTS OF THE HUBBARD MODEL	31
4.2	THE ONE-DIMENSIONAL HUBBARD MODEL AND EXPERIMENTS	34
4.3	SYMMETRIES IN THE HUBBARD MODEL	35
4.4	COMPOSITE SYSTEMS FOR THE HUBBARD MODEL	37
4.5	DMRG FOR THE HUBBARD CHAIN	40
4.6	RESULTS	40
4.6.1	DISCUSION	41
5	AN ELECTRON-PHONON INTERACTION HAMILTONIAN	48
5.1	LARGE NUMBER OF DEGREES OF FREEDOM	49
5.2	ANOMALIES IN $\text{YBa}_2\text{Cu}_3\text{O}_{7-\delta}$	50
5.3	GENERALIZATION TO A FINITE SIZE CHAIN	53
5.4	RESULTS	54
5.5	THE PSEUDOSITES APPROACH	57
5.5.1	THE MAPPING TO PSEUDOSITES	60
5.5.2	RESULTS	62
6	CONCLUSIONS AND PERSPECTIVES	65
A	THE OPTIMAL STATES	67

LIST OF FIGURES

3.1	FIRST STEPS IN THE INFINITE SYSTEM ALGORITHM.	21
3.2	THE INFINITE SYSTEM SCHEME.	21
3.3	THE INFINITE SIZE PREVIOUS TO THE FINITE SIZE SYSTEM ALGORITHM.	23
3.4	FINITE SYSTEM SCHEME.	24
3.5	L SITES.	26
3.6	THE STATE OF THE SYSTEM.	27
3.7	TWO SITES	28
3.8	THE SUPERBLOCK.	28
3.9	SYSTEM AND ENVIRONMENT.	29
4.1	CONFIGURATION FOR A HUBBARD CHAIN.	33
4.2	FOUR SITES SYSTEM.	39
4.3	DMRG VS BETHE ANZAT	43
4.4	ENERGY PER SITE.	44
4.5	ENERGY VS N_e	45
4.6	ENERGY VS U/T	46
5.1	$YBa_2Cu_3O_7$	51
5.2	ENERGY VS NUMBER OF SITES.	56
5.3	REPLACEMENT OF BOSON STATES BY PSEUDOSITES.	57
5.4	GROWING OF A PSEUDOSITES SYSTEM.	60
5.5	EIGENVALUES OF THE ELECTRONIC SPACE.	63
5.6	GROUND STATE OF THE ELECTRON-PHONON SYSTEM	63
5.7	ENERGY AS A FUNCTION OF λ_{IR}	64

LIST OF TABLES

4.1	<i>Comparison of the ground state energy for the Hubbard model obtained from eq. (4.5) and the obtained by DMRG for a 16 sites chain at half filling and $S_z = 0$.</i>	42
4.2	<i>Comparison of our results with a low number of retained states with those obtained by DMRG in momentum space in [21].</i>	42
5.1	<i>The ground state energy for several sizes maintaining the ratio charge-size fixed to 2/3. L is the size and Q the charge corresponding to the energy E.</i>	55

RESUMEN

En esta tesis hemos aplicado el método de renormalización de grupo de la matriz densidad¹ a un Hamiltoniano que introduce grados de libertad fonónicos, con el fin de entender al acoplamiento electrón-fonón que ocurre en los superconductores cerámicos de alta temperatura. El trabajo se basa en resultados previos publicados en el campo [27, 28, 32, 34]. La investigación se enfoca en la energía de estado base y se exploran varios regímenes del acoplamiento electrón-fonón. Los sistemas físicos considerados aquí son cadenas de iones de oxígeno y cobre. Las cadenas de menor tamaño consisten de tres sitios que aparecen como cadenas aisladas en el cerámico $\text{YBa}_2\text{Cu}_3\text{O}_7$. Aquí se han explorado dos aproximaciones al estudio de sistemas bosónicos, la base fonónica óptima y el método de pseudositos. Como complemento, se ha investigado el caso simple del modelo de Hubbard unidimensional.

Palabras clave: Renormalización de grupo, Matriz densidad, Interacción electrón-fonón, Superconductores de alta temperatura, Modelo de Hubbard.

¹Usaremos el acrónimo DMRG en adelante

ABSTRACT

In this thesis we apply the density matrix renormalization group² method to a Hamiltonian which introduces phononic degrees of freedom with the aim of understanding the electron-phonon coupling occurring in ceramic high T_c superconductors. The work is supported on previous published results in the field [27, 28, 32, 34]. The investigation focuses on the ground state energy exploring several regimes of the electron phonon coupling. The physical systems considered here are Oxygen-Copper chains. The lowest size chains are the three site O-Cu-O clusters which appear as isolated chains in $\text{YBa}_2\text{Cu}_3\text{O}_7$. Here, we explore two approaches for studying boson systems, the Optimal Phonon Basis and the Method of Pseudospins. As a complement, the simplest case of the one-dimensional Hubbard model is investigated.

Key words: Group renormalization, Density matrix, electron-phonon interaction, High temperature superconductors, Hubbard model.

²We shall use the acronym DMRG hencefort

PREFACE

The present thesis is delivered as a requirement to obtain the Applied Sciences Master degree within the Advanced Materials Program at the Instituto Potosino de Investigación Científica y Tecnológica (IPICYT). The work was developed at the installations of the Advanced Materials Department in IPICYT under the supervision of Professor Aldo H. Romero (CINVESTAV-QTRO) and in collaboration with Professor Jereson Silva (National University of Colombia).

The thesis is concerned with the DMRG method, a powerful numerical technique widely tested in many studies of the properties of one dimensional quantum systems which we apply here with the aim of getting relevant information about the superconductivity phenomena in ceramic superconductors.

This work represents a very ambitious project because it involves the knowledge of a technique that despite being easy to understand, demands a variety of technicalities and programming abilities to elaborate a good program. Furthermore, for the problem we are interested in it is necessary to adapt the algorithms to improve the efficiency and because the physical system we deal with is of inhomogeneous kind. In addition, some superconductivity theory background is needed and it becomes harder principally because the problem is not yet totally understood.

The thesis promises to be a good support for anybody who wants to initiate working in the DMRG methodology because it present some details avoided in the majority of the publications on the topic and more explanations are included for those who know nothing.

José Manuel Nápoles Duarte.

March, 2006

Chapter 1

Introduction

According to many textbooks, such as Aschroft and Mermin [1], many problems in condensed matter physics can be described within a single-particle picture. When the weak effective framework breaks down, we pass to the field of strongly correlated quantum systems, where the full electronic many body problem has to be treated. In general, the description of a many body quantum system involves a huge number of degrees of freedom which increases exponentially with size. While this kind of systems should be described by the Schrödinger equation, its explicit solution may be hard to find. To study strongly correlated systems, simplified model Hamiltonians have been designed that try to retain just the core ingredients needed to describe some physical phenomenon. They are usually Spin and Fermion Hamiltonians. Symmetry properties and the knowledge of quantum numbers have been used to reduce the numerical effort in calculations but even in this case the task becomes prohibitive.

Recent progress has been made by means of the DMRG approach, a numerical technique introduced in 1992 by Steven White [14] and related skins [23,24,40]. In particular, for quantum systems in one spatial dimension and short range interactions, DMRG provides high accuracy approximations to the ground state, the low lying excited states, and to the spectral properties at a really modest computational effort [15, 18].

In the present work, the DMRG is used to study the one-dimensional Holstein-

Hubbard like Hamiltonians which are of interest in the superconductivity field. The form of the Hamiltonian studied which is studied is that introduced in [34] for a three-site cluster. It contains an electronic part, including electronic correlations, a phononic part, and a charge lattice interaction terms. The Hamiltonian, with the particular three-sites configuration, was used to describe the local dynamics of the O(4)-Cu(1)-O(4) cluster, which bridges between the CuO₂ planes in YBa₂Cu₃O₇, and also to infer polaronic behavior within this cluster.

We have chosen to work with two approaches for the systems possessing boson degrees of freedom, namely the optimal phonon basis [24] and the method of pseudosite [23]. Both approaches were designed to treat systems including bosons, and imply the dealing with large Hilbert spaces.

1.1 Outline of the thesis

This Thesis is organized as follows: The second chapter presents a brief survey to several basic quantum mechanical concepts is included with the goal to establish the terminology that we use later. The key ones are the formalism of second quantization for bosons and fermions and the existence of conserved quantities leading to the simplification of the calculations in the Hilbert space.

The third chapter starts with a presentation of the basics of the DMRG method following the original paper of White [14]. Then, the two main algorithms for the effective implementation of any DMRG calculation are discussed. In addition, some hints are given of how to proceed for a preliminary implementation in the case of a linear chain.

In the four chapter, we introduce the Hubbard model which presents two advantages; first it allows to exemplify how one need to proceed in the implementation of DMRG and second because it is convenient to understand the electronic interacting contribution of a Hamiltonian introduced in order to explain some su-

1.1. Outline of the thesis

perconductivity behavior.

Finally, in the fifth chapter we present the main contribution of this thesis: the application of DMRG to an electron-phonon interaction Hamiltonian which models an inhomogeneous system composed of copper and oxygen alternated atoms in a one dimensional chain. Here we focused only on obtaining the ground state in the different parameterizations.

Chapter 2

Quantum Mechanics: A Brief Review

2.1 Quantum states, operators and their main properties

A quantum mechanical system is defined by a Hilbert space \mathcal{H} whose vectors are states that we denote by using Dirac's notation being $|\psi\rangle$ a ket and $(|\psi\rangle)^* = \langle\psi|$ a bra. There are linear operators which act on this Hilbert space. These operators correspond to physical observable. Also, an inner product is defined, which assigns a complex number, $\langle\psi|\phi\rangle$ to any pair of states $\langle\psi|$ and $|\phi\rangle$.

A state vector $|\psi\rangle$ gives a complete description of a system through the expectation values of a complete set of operators of the form $\langle\psi|O|\psi\rangle$ (assuming that $|\psi\rangle$ is normalized to unity, i.e. $\langle\psi|\psi\rangle = 1$).

If for all vectors $|\psi\rangle$ and $|\phi\rangle$ belonging to a given Hilbert space, we have

$$\langle\phi|L|\psi\rangle = \langle\psi|O|\phi\rangle^*, \quad (2.1)$$

where $*$ denotes complex conjugate, then the operator L is the Hermitian adjoint of O and will be denoted by O^\dagger . Moreover, the so-called Hermitian operators satisfies

$$O = O^\dagger, \quad (2.2)$$

2.1. Quantum states, operators and their main properties

while a unitary operator satisfies

$$OO^\dagger = O^\dagger O = I \quad (2.3)$$

where I is the identity matrix. For any linear operator, is very important the eigenvalue problem, i.e.,

$$O|\psi\rangle = \lambda|\psi\rangle \quad (2.4)$$

where λ are complex numbers called eigenvalues and $|\psi\rangle$ are the eigenvectors or eigenstates of O . The Hermitian operators have the very important propertie that their eigenvalues are real. An interesting property of Hermitian operators, is that its eigenstates $\{|\psi\rangle\}$ are orthogonal between them

$$\langle\phi|O|\psi\rangle = \lambda\langle\phi|\psi\rangle = \lambda'\langle\psi|\phi\rangle, \quad (2.5)$$

for $\lambda \neq \lambda'$

$$\langle\phi|\psi\rangle = 0. \quad (2.6)$$

Hence, the eigenstates $\{|\psi\rangle\}$ can be used as a basis for Hilbert space. This mean that any state $|\Phi\rangle$ can be expanded in the basis given by the eigenstates of O :

$$|\Phi\rangle = \sum_{\psi} c_{\psi} |\psi\rangle, \quad (2.7)$$

with $c_{\psi} = \langle\psi|\Phi\rangle$. From eq.(2.7) another characteristic of any given state can be observed, they can be written as vectors by taking the coefficients c_{ψ} of the expansion in (2.7) as the entries of a column vector. This is due to a mathematical field called Group representation. Representation theory is important because it enables many group-theoretic problems to be reduced to problems in linear algebra, which is a very well-understood theory. For instance if a basis has two states $\{|\uparrow\rangle, |\downarrow\rangle\}$, the two eigenstates might be defined in terms of vectors as follows

$$|\uparrow\rangle = \begin{pmatrix} 1 \\ 0 \end{pmatrix}, \quad |\downarrow\rangle = \begin{pmatrix} 0 \\ 1 \end{pmatrix}, \quad (2.8)$$

by noting that

$$|\uparrow\rangle = 1|\uparrow\rangle + 0|\downarrow\rangle \quad (2.9)$$

and

$$|\downarrow\rangle = 0|\uparrow\rangle + 1|\downarrow\rangle, \quad (2.10)$$

where $|\uparrow\rangle$ and $|\downarrow\rangle$ can be considered as the eigenstates of S_z , the spin operator in the z direction.

Furthermore any operator can be described in terms of both bras and kets as follows

$$O = \sum_{\lambda\lambda'} a_{\lambda\lambda'} |\lambda\rangle\langle\lambda'|. \quad (2.11)$$

Just as any state can be equivalently expressed as a vector, any operator can be expressed by a matrix with entries

$$O_{\lambda\lambda'} = \langle\lambda|O|\lambda'\rangle. \quad (2.12)$$

For example, in the representation of spin, the S_z operator can be written as

$$S_z = \frac{\hbar}{2} |\uparrow\rangle\langle\uparrow| - \frac{\hbar}{2} |\downarrow\rangle\langle\downarrow|, \quad (2.13)$$

whereas in the matrix form as

$$S_z = \begin{array}{c} \langle\uparrow| \\ \langle\downarrow| \end{array} \begin{array}{cc} |\uparrow\rangle & |\downarrow\rangle \\ \left(\begin{array}{cc} \frac{\hbar}{2} & 0 \\ 0 & -\frac{\hbar}{2} \end{array} \right) \end{array}. \quad (2.14)$$

2.2 Invariance in quantum mechanics

The concept of invariance is in often useage in quantum mechanics. Invariance means at the quantum level that an operator remains the same after an application of unitary transformations of the type:

$$H = U^{-1}HU, \quad (2.15)$$

2.3. More on eigenvalue problems

or equivalently

$$[H, U] = 0, \quad (2.16)$$

with respect to a group of transformations, the whole Hilbert space is decomposed in invariant subspaces, that is there are subsets of vector states from the basis that under the action of a given operator they transform to the same subset as follows

$$|\psi'\rangle = U|\psi\rangle \quad (2.17)$$

where $|\psi'\rangle$ and $|\psi\rangle$ belong to a given subset. The group of operators that satisfy this equation form a group representation. Suppose Γ is a Hermitian operator, corresponding to a physical observable, which is invariant under a group representation of transformations. It follows that Γ commutes with the group of operators $\mathfrak{G} = \{T, S, \dots\}$

$$[\Gamma, T] = 0, \quad [\Gamma, S] = 0, \quad \dots \quad (2.18)$$

Suppose γ is a N -fold degenerate eigenvalue of Γ , i.e., there exists a N -dimensional manifold \mathfrak{M} in the Hilbert space such that all vectors of \mathfrak{M} are eigenvectors of Γ belonging to the eigenvalue γ . If $|\psi\rangle$ is any vector of \mathfrak{M} and T an operator of the group \mathfrak{G} , it follows that

$$\Gamma(T|\psi\rangle) = T\Gamma|\psi\rangle = T\gamma|\psi\rangle = \gamma(T|\psi\rangle) \quad (2.19)$$

i.e., $(T|\psi\rangle)$ is also an eigenvector of Γ belonging to the same eigenvalue γ , i.e. it also lies in \mathfrak{M} . Hence \mathfrak{M} is an invariant manifold of the group \mathfrak{G} : *operators of \mathfrak{G} transform vectors of \mathfrak{M} into vectors of \mathfrak{M} .*

2.3 More on eigenvalue problems

Let us assume that we have already solved the eigenvalue problem of a Hermitian operator A , i.e., we know the eigenvalues a_1, a_2, \dots, a_n and correspondingly the complete set of its orthonormal eigenfunctions $|\psi_1\rangle, |\psi_2\rangle, \dots, |\psi_n\rangle$. If we take this set of eigenfunctions as basis of a matrix representation of A , it follows from

$$\langle\psi_i|A|\psi_j\rangle = a_j\langle\psi_i|\psi_j\rangle = a_j\delta_{ij} \quad (2.20)$$

that the matrix A is a diagonal matrix with the eigenvalues of A on the diagonal

$$A = \begin{pmatrix} a_1 & 0 & 0 & \cdots \\ 0 & a_2 & 0 & \cdots \\ 0 & 0 & a_3 & \vdots \\ \vdots & \vdots & \cdots & \ddots \end{pmatrix}. \quad (2.21)$$

Though by a suitable choice of eigenfunctions we can always diagonalize A , degenerate eigenfunctions belonging to the same eigenvalue will not be orthogonal. Hence, in this case A will not be diagonal, but consisting of blocks, containing non-zero elements, arranged along the principal diagonal.

The eigenfunctions labeling the rows and columns of any block belong to the same eigenvalue. They span the corresponding manifold in Hilbert space. We illustrate this for a four dimensional space $a_1 = a_2 \neq a_3 = a_4$

$$A = \left(\begin{array}{cc|cc} A_{11} & A_{12} & & 0 \\ A_{21} & A_{22} & & 0 \\ \hline & & A_{33} & A_{34} \\ & & A_{43} & A_{44} \end{array} \right). \quad (2.22)$$

where $A_{ij} = a_1 = a_2$ for $i, j = 1, 2$ and $A_{ij} = a_3 = a_4$ for $i, j = 3, 4$.

2.4 Composite Systems

If a system is composed of subsystems A and B which have as associated Hilbert spaces \mathcal{H}_A and \mathcal{H}_B , then the associated Hilbert space of the joined system is the tensor product space $\mathcal{H}_A \otimes \mathcal{H}_B$, and it is called the composite system"

If subsystem A is in state $|\psi\rangle$ and subsystem B is in state $|\phi\rangle$, then the joint system is in the product state $|\psi\rangle \otimes |\phi\rangle$.

If U_A is a unitary transformation which acts on subsystem A , then $U_A \otimes I_B$ is the corresponding unitary transformation for the joint system. Similarly, if U_B acts on B , then $I_A \otimes U_B$ is the unitary transformation for the joint system.

2.5. Second quantization

If O_A is an observable for subsystem A , then $O_A \otimes I_B$ is the corresponding observable for the joint system; and similarly for O_B on B and $I_A \otimes O_B$ on the joint system. Note that $O_A \otimes I_B$ and $I_A \otimes O_B$ always commute, and therefore are compatible observables¹.

2.5 Second quantization

The procedure of second quantization is often used to describe many particle systems. In general, any problem in solid state theory can be reduced to the dynamics of a set of excitations from a ground state. To manage this picture, the method of second quantization is one of the best choices. Basically it is the representation of quantum states of a system in the number of particles or excitations occupying a given state. Any state $|\Psi\rangle$ of a system of identical particles is a linear combination of many particle basis states $\{|\phi\rangle\}$ as follows

$$|\Psi\rangle = \sum_j c_j |\phi_j\rangle. \quad (2.23)$$

A basis state can be completely specified in terms of the occupation number n_α for each member of a complete set of orthonormal single-particle states, $\{|\alpha\rangle, \alpha = 1, 2, 3, \dots\}$. The set of occupation numbers contains all the information required to construct an appropriately symmetrized or antisymmetrized basis vector depending on the bosonic or fermionic character of the excitation, this can be denoted by:

$$|\Psi\rangle = |n_1, n_2, \dots, n_\alpha, \dots\rangle, \quad (2.24)$$

where n_α is the number of particles or excitations occupying a "single-particle" state.

For bosons, n_α must be a non-negative integer whereas for fermions, the famous Pauli exclusion principle restricts each of the n_α to be either 0 or 1.

¹Physically, this means that measurements on different subsystems can always be done simultaneously.

The vector space spanned by the set of occupation number basis states is called the Fock space. A feature of the Fock space is that the total number of particles is not a fixed parameter, but rather a dynamical variable associated with a total number operator

$$N = \sum_{\alpha} n_{\alpha}. \quad (2.25)$$

Moreover, there is a unique vacuum or zero-particle state:

$$|0\rangle = |0, 0, 0, \dots\rangle, \quad (2.26)$$

usually taken as the ground state of the many-body system under specific consideration.

The single particle states can be represented as

$$|\alpha\rangle = |0_1, 0_2, \dots, 0_{\alpha-1}, 1_{\alpha}, 0_{\alpha+1}, \dots\rangle \quad (2.27)$$

2.5.1 Bosonic operators

Let us define the bosonic creation operator a_{α}^{\dagger} in the standard way:

$$a_{\alpha}^{\dagger} |n_1, n_2, \dots, n_{\alpha-1}, n_{\alpha}, n_{\alpha+1}, \dots\rangle = \sqrt{n_{\alpha} + 1} |n_1, n_2, \dots, n_{\alpha-1}, n_{\alpha} + 1, n_{\alpha+1}, \dots\rangle \quad (2.28)$$

and the corresponding annihilation operator a_{α} by

$$a_{\alpha} |n_1, n_2, \dots, n_{\alpha-1}, n_{\alpha}, n_{\alpha+1}, \dots\rangle = \sqrt{n_{\alpha}} |n_1, n_2, \dots, n_{\alpha-1}, n_{\alpha} - 1, n_{\alpha+1}, \dots\rangle \quad (2.29)$$

With these two operators one can define a number operator $N_{\alpha} = a_{\alpha}^{\dagger} a_{\alpha}$, such that

$$N_{\alpha} |n_1, n_2, \dots, n_{\alpha}, \dots\rangle = n_{\alpha} |n_1, n_2, \dots, n_{\alpha}, \dots\rangle \quad (2.30)$$

and

$$N = \sum_{\alpha} N_{\alpha} \quad (2.31)$$

The simplest application of the creation and annihilation operators involves the single-particle states:

$$a_{\alpha}^{\dagger} |0\rangle = |\alpha\rangle, \quad a_{\alpha} |\beta\rangle = \delta_{\alpha,\beta} |0\rangle \quad (2.32)$$

2.5. Second quantization

When applied to many-particle states, the properties of the creation and annihilation operators must be consistent with the symmetry of bosonic states under pairwise interchange of particles. We can see from eqs. (2.28) and (2.29) that for any pair of single particle states $|\alpha\rangle$ and $|\beta\rangle$ and for any vector Ψ in the Fock space, that we have the relationships: $a_\alpha^\dagger a_\beta^\dagger |\Psi\rangle = a_\beta^\dagger a_\alpha^\dagger |\Psi\rangle$ and $a_\alpha a_\beta |\Psi\rangle = a_\beta a_\alpha |\Psi\rangle$. One also finds that $a_\alpha^\dagger a_\beta |\Psi\rangle = a_\beta a_\alpha^\dagger |\Psi\rangle$ for $\alpha \neq \beta$. However, $a_\alpha^\dagger a_\alpha |\Psi\rangle = n_\alpha$ while $a_\alpha a_\alpha^\dagger |\Psi\rangle = (n_\alpha + 1)|\Psi\rangle$. This means that for any $|\Psi\rangle$ in the Fock space

$$a_\alpha a_\alpha^\dagger |\Psi\rangle - a_\alpha^\dagger a_\alpha |\Psi\rangle = (n_\alpha + 1)|\Psi\rangle - n_\alpha |\Psi\rangle = |\Psi\rangle \quad (2.33)$$

The latter properties can be summarized through the commutation relations

$$[a_\alpha^\dagger, a_\beta^\dagger] = [a_\alpha, a_\beta] = 0, \quad [a_\alpha, a_\beta^\dagger] = \delta_{\alpha,\beta} I \quad (2.34)$$

One consequence of these commutation relations is that any many-particle basis state can be written as a multiple excitation of the vacuum state as follows:

$$|n_1, n_2, \dots, n_\alpha, \dots\rangle = (a_1^\dagger)^{n_1} (a_2^\dagger)^{n_2} \dots (a_\alpha^\dagger)^{n_\alpha} \dots |0\rangle \quad (2.35)$$

or equally well, as any permutation of the above product of operators acting on the vacuum. For example

$$|2, 1, 0, 0, \dots, 0\rangle = a_1^\dagger a_1^\dagger a_2^\dagger |0\rangle = a_1^\dagger a_2^\dagger a_1^\dagger |0\rangle = a_2^\dagger a_1^\dagger a_1^\dagger |0\rangle \quad (2.36)$$

We stress that the eqs. (2.28), (2.29) and (2.34) define the key properties of bosonic creation and annihilation operators.

2.5.2 Fermionic operators

In the fermionic case we have to require antisymmetry under all possible pairwise interchanges. We define the fermionic creation operator c_α^\dagger as follows:

$$\begin{aligned} c_\alpha^\dagger |n_1, n_2, \dots, n_{\alpha-1}, 0_\alpha, n_{\alpha+1}, \dots\rangle &= (-1)^{\nu_\alpha} |n_1, n_2, \dots, n_{\alpha-1}, 1_\alpha, n_{\alpha+1}, \dots\rangle \\ c_\alpha^\dagger |n_1, n_2, \dots, n_{\alpha-1}, 1_\alpha, n_{\alpha+1}, \dots\rangle &= 0, \end{aligned} \quad (2.37)$$

and the annihilation operator c_α by

$$\begin{aligned} c_\alpha |n_1, n_2, \dots, n_{\alpha-1}, 1_\alpha, n_{\alpha+1}, \dots\rangle &= (-1)^{\nu_\alpha} |n_1, n_2, \dots, n_{\alpha-1}, 0_\alpha, n_{\alpha+1}, \dots\rangle \\ c_\alpha |n_1, n_2, \dots, n_{\alpha-1}, 0_\alpha, n_{\alpha+1}, \dots\rangle &= 0, \end{aligned} \quad (2.38)$$

In both eqs. (2.37) and (2.38)

$$\nu_\alpha = \sum_{\beta < \alpha} N_\beta, \text{ where } N_\beta = c_\beta^\dagger c_\beta \quad (2.39)$$

measures the total number of particles in single-particle states having an index $\beta < \alpha$. It is straightforward to check that eqs. (2.37), (2.38) and (2.39) are self-consistent, in the sense that with the phase factor $(-1)^{\nu_\alpha}$ as already defined,

$$N_\alpha |n_1, n_2, \dots, n_\alpha, \dots\rangle = n_\alpha |n_1, n_2, \dots, n_\alpha, \dots\rangle \text{ for } n_\alpha = 0 \text{ or } 1. \quad (2.40)$$

From these equations, it is clear that for any $|\Psi\rangle$, $c_\alpha^\dagger c_\beta^\dagger |\Psi\rangle = -c_\beta^\dagger c_\alpha^\dagger |\Psi\rangle$ for $\alpha \neq \beta$, while $c_\alpha^\dagger c_\alpha^\dagger |\Psi\rangle = -c_\alpha^\dagger c_\alpha^\dagger |\Psi\rangle = 0$. Similarly, $c_\alpha c_\beta |\Psi\rangle = -c_\beta c_\alpha |\Psi\rangle$ for $\alpha \neq \beta$, and $c_\alpha c_\alpha |\Psi\rangle = 0$.

We also have $c_\alpha^\dagger c_\beta |\Psi\rangle = -c_\beta c_\alpha^\dagger |\Psi\rangle$ for $\alpha \neq \beta$. However, $c_\alpha^\dagger c_\alpha |\Psi\rangle = n_\alpha |\Psi\rangle$ for any basis state Ψ , whereas $c_\alpha c_\alpha^\dagger |\Psi\rangle = (1 - n_\alpha) |\Psi\rangle$. Thus

$$(c_\alpha c_\alpha^\dagger + c_\alpha^\dagger c_\alpha) |\Psi\rangle = (1 - N_\alpha) |\Psi\rangle + N_\alpha |\Psi\rangle = |\Psi\rangle \quad (2.41)$$

for any $|\Psi\rangle$ in the Fock space.

Again, the afore mentioned properties can be summarized in the anticommutation relations

$$\{c_\alpha^\dagger, c_\beta^\dagger\} = \{c_\alpha, c_\beta\} = 0, \quad \{c_\alpha, c_\beta\} = \delta_{\alpha,\beta} I \quad (2.42)$$

where $\{A, B\} = AB + BA$ is the anticommutator of A and B . These anticommutation properties distinguish in a fundamental manner the fermionic operators from their commuting bosonic counterparts. The phase factors $(-1)^{\nu_\alpha}$ entering eqs. (2.37) and (2.38) were specifically chosen to ensure that eqs. (2.42) are satisfied.

2.5. Second quantization

Once given the anticommutation relations, any many-particle basis state can be written in the following way:

$$|n_1, n_2, \dots, n_\alpha, \dots\rangle = (c_1^\dagger)^{n_1} (c_2^\dagger)^{n_2} \dots (c_\alpha^\dagger)^{n_\alpha} \dots |0\rangle \quad (2.43)$$

or equally well, as any permutation of the above product of creation operators with a sign change for each pairwise interchange of adjacent operators. For example

$$|1, 1, 1\rangle = c_1^\dagger c_2^\dagger c_3^\dagger |0\rangle = c_2^\dagger c_1^\dagger c_3^\dagger |0\rangle = c_2^\dagger c_3^\dagger c_1^\dagger |0\rangle = c_3^\dagger c_2^\dagger c_1^\dagger |0\rangle = c_3^\dagger c_1^\dagger c_2^\dagger |0\rangle = c_1^\dagger c_3^\dagger c_2^\dagger |0\rangle \quad (2.44)$$

eqs. (2.37), (2.38) and (2.42) define the key properties of fermionic creation and annihilation operators.

Chapter 3

The DMRG Method

The DMRG method is a powerful numerical technique for studying many body systems, particularly well-suited for systems of low dimensionality. It has been developed by Steven White during 1992 with the aim of avoiding the problems arising from the application of Numerical Renormalization methods for the Kondo problem [13, 14]. It consist of a systematic truncation of the Hilbert space using a unitary transformation to a basis formed by the eigenvectors of the reduced density matrix of a subsystem in the entire system of study.

In this thesis, we apply the DMRG methodology to one dimensional systems. This chapter is devoted to the introduction of this method and we decide to divide the discussion into two sections. The first one is an overview of the basics of DMRG. The two algorithms corresponding to the cases of a infinite system and of a finite one are shortly commented. The second and last section of this chapter is a hint to the reader about the way DMRG can be implemented.

3.1 Basics on DMRG

The behavior of a quantum mechanical system is, in general, governed by the time-dependent schrödinger equation:

$$i\hbar\frac{\partial}{\partial t}|\psi(t)\rangle = H|\psi(t)\rangle \quad (3.1)$$

or its time-independent form

$$H|\psi\rangle = E|\psi\rangle, \quad (3.2)$$

where $|\psi\rangle$ is a state in the Hilbert space and H is the Hamiltonian operator, expressed as a function of creation and annihilation operators. One approach to treating quantum mechanical systems numerically is to solve the eigenvalue problem formed by the Hamiltonian of the system. Note that Hamiltonians without interaction, i.e., consisting of a sum of single-particle terms, can be solved by treating the single-particle problem with no need to work in the full many body basis. However, for systems with strong interactions it is not possible to reduce the problem to a single particle problem. In such cases, the full many body problem has to be taken into account. Standard way to numerically investigate a physical system is to discretize the underlying differential equation or to map the model onto or formulate it directly on a lattice. It is then necessary to describe model properties on the lattice sites (specifying if it is a spin system or if the particles are fermions or bosons.). The system is then composed of N quantum mechanical subsystems, with each subsystem located on a site j and described by a (usually finite) number of basis states which depend on the model and may vary from site to site. Roughly speaking, one can classify the models of interest as fermionic or bosonic lattice models, as pure spin models, and as impurity models. To model a regular solid, one usually works within the Born-Oppenheimer approximation, i.e., one assumes the atomic nuclei as moving slowly enough so that they can be considered to be fixed on the relevant time scale for the electronic problem. The simplest fermionic lattice model is the tight-binding model, which treats electrons as being localized to Wannier-orbitals centered on a regular array of sites. Such a model would be appropriate for unfilled d or f orbitals in transition metals, for example. In the simplest case, one restricts the description to only a single band, although multi-band models can also be considered. Due to the finite overlap between nearby orbitals, the particle can hop, from one site to another, i.e. tunnel between the corresponding Wannier nearby orbitals with an amplitude denoted by t [41]. If the lattice has n sites and there are k possible states per site, then the dimension of the Hilbert space is k^n . Assuming a Tight-Binding lattice model we

3.1. Basics on DMRG

have local orbitals on each site which can take $k = 4$ different states of up to two electrons ($|0\rangle, |\uparrow\rangle, |\downarrow\rangle, |\uparrow\downarrow\rangle$). When n is large enough the eigenvalue problem is out of the capability of any human or computer means. These facts open the door to a variety of approximate methods, among which the renormalization group (RG) approach, especially when combined with other techniques (e.g. numerical, variational, etc.), is one of the most relevant.

The main idea of the RG method is the mode elimination or reduction of the degrees of freedom followed by an iteration which reduces the number of variables, step by step, until a more manageable situation is reached [17]. The standard real-space RG approach consists of considering a group of sites to be a "block", and diagonalizing that block to find a set of eigenstates. One then truncates the set of eigenstates, keeping only the lowest m states (ordered by energy), and uses those states to construct an approximate Hamiltonian for a new, larger block composed of two of the previous blocks [13]. One assumes when using this procedure that only the lowest-lying block eigenstates play a dominant role in forming states of larger blocks at later iterations [14].

Although the eigenstates of an effective block Hamiltonian are natural states to use in the approach, they are not optimal. In particular, because its eigenstates have inappropriate features at the block edges. They are optimal only in the limit that the connections to other blocks vanish [14].

In the following we explain how DMRG works. We hope to do this as pedagogical as we can, even though we recommend the reader the first chapters of reference [4] and also chapter VII of reference [3] for specific details.

First, consider a finite-size quantum lattice which *we can diagonalize exactly*. A convenient basis for the Hilbert space of such a system has states of the form [3]

$$|1\rangle \otimes |2\rangle \otimes \cdots \otimes |n\rangle \quad (3.3)$$

where $|s\rangle$ labels a state of a single site of the system, and \otimes denotes a tensorial product. If there are k possible states per site, then the Hilbert space dimension is k^n [3]. For example in the simple spin 1/2 Heisenberg model, there are two possible states per site, say $|\uparrow\rangle$ and $|\downarrow\rangle$. With this basis, we can form explicitly

the matrix Hamiltonian¹ and obtain the ground state eigenvector $|\Psi\rangle$. Now, we call the full system the superblock and divide into two parts, say the system block and the environment block.

Let $|i\rangle$ label the states describing the system block and $|j\rangle$ label the states for the environment. Then the ground state of the system can be expanded as a product state of the system and the environment as

$$|\Psi\rangle = \sum_{ij} \Psi_{ij} |i\rangle |j\rangle. \quad (3.4)$$

We wish to generate a set of optimal states for the system block which are especially appropriate to represent its properties when the superblock is in the state $|\Psi\rangle$. It is possible to show that these optimal states are the largest eigenvalue eigenvectors of the reduced density matrix [14]. If the superblock is in the pure state $|\Psi\rangle$, the density matrix is defined as

$$\begin{aligned} \rho &= |\Psi\rangle\langle\Psi| \\ &= \sum_{ij} \psi_{ij} |i\rangle |j\rangle \sum_{i'j'} \psi_{i'j'}^* \langle i' | \langle j' |, \end{aligned} \quad (3.5)$$

whereas the reduced density matrix for the system block is obtained by tracing out through the states of the environment block:

$$\begin{aligned} \rho_{red} &= Tr_E |\psi\rangle\langle\psi| \\ &= \sum_j \langle j | \rho | j \rangle \\ &= \sum_j \sum_i \sum_{i'} \psi_{ij} \psi_{i'j}^* |i\rangle \langle i'|, \end{aligned} \quad (3.6)$$

so that the matrix elements of ρ_{red} are given by

$$\rho_{ii'} = \sum_j \psi_{ij} \psi_{i'j}^*. \quad (3.7)$$

In the following we denote ρ_{red} simply by ρ as we do not use the density matrix but the reduced density matrix.

¹as in sec. (2.1)

3.1. Basics on DMRG

The DMRG allows for a systematic truncation of the Hilbert space by keeping the most probable states describing a wave function instead of the lowest energy states usually kept in previous real space renormalization techniques. The basic idea of DMRG is the same of the RG methods and consists in beginning with a small system that can be handled exactly. The system size is then increased *without increasing the dimension of the Hilbert space* until the desired system size is reached. This is perhaps the most important contribution of the RG methods because the dimension of the Hilbert space of any system grows exponentially with the size. Thus the procedures of diagonalization becomes prohibitive for any computer workstation. The principal contribution of DMRG is that the basis used in each renormalization step is the optimal basis for such step.

3.1.1 DMRG algorithms

The implementation of the DMRG can be done into two forms, through the known as infinite system method or through the finite system method [15]. The infinite size algorithm begins with a system small enough to be solved from numerical methods such as exact diagonalization. Then one apply a iterative procedure described below, until the system is large enough to represent properties of the infinite system. Usually the size is previously defined and the goal is to represent that system with the approximation of the infinite size algorithm. When the desired size is reached, one can apply the second method which works with the resultant superblock formed in the last iteration of the infinite size algorithm, improving its approach. In this section we describe these algorithms originally proposed by S. White [15].

Infinite size algorithm

In the first step of the infinite size algorithm one start with a four sites chain and systematically increase the size of the chain by adding two sites until the desired

size is reached². The most common way to do this is by making a system as part of a whole block, called super block, and making the environment as a reflection of the system; Then at each time a site is added to the system and this joint is relabeled as the system block which lead to a new environment. The operators related to the system block and to the environment block are transformed to the basis of a reduced density matrix for the system block. In the implementation these eigenvectors are hold in a matrix, say O and then a unitary transformation is performed with O and O^\dagger . The infinite system algorithm could be summarized as follows:

1. Make a four site system which is the initial superblock. Label the first site system block and the last environment block (see fig. 3.1).
2. Form the Hamiltonian matrix for the superblock
3. diagonalize it with a sparce matrix diagonalization algorithm to find the ground state (actually could be an exited state but we are interested in the ground state properties).
4. form a reduced density matrix for the system block plus a site. Hold only the m largest eigenvectors.
5. relabel the join of the system plus a site as the system block. Add also a site to the environment and relabel it as the environment block.
6. Form the transformation matrices O with the selected eigenvectors arranged in columns. Form also O^\dagger .
7. Transform the operators for the system to the reduced basis with O and O^\dagger .
8. Build a new superblock with the system block, two single sites and the environment.
9. go to step 2.

²or other manageable size

3.1. Basics on DMRG

The infinite size system algorithm is illustrated in fig. 3.2.

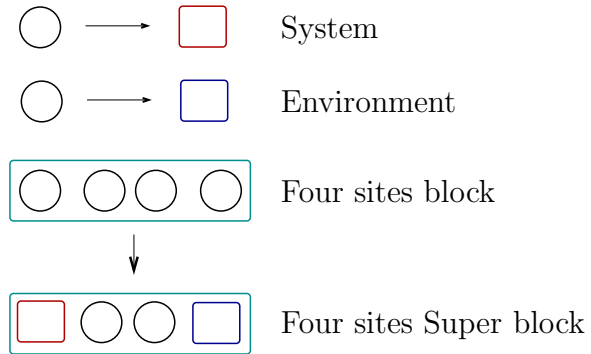


Figure 3.1: *Initially the system and environment consists of one site each one. Then two sites are added between them to form a 4 sites block which might be the first superblock.*

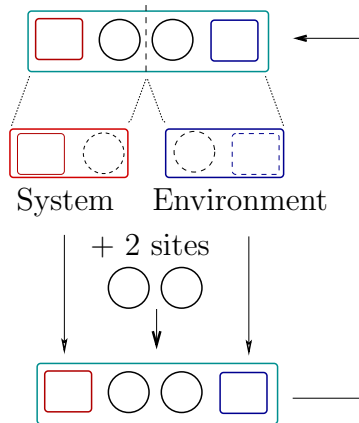


Figure 3.2: *The iterative procedure requires the formation of a new superblock from a previous one. System and environment re defined and two new sites are introduced.*

finite size algorithm

The finite size system algorithm begins with the super block builded in the last iteration of the infinite size system. It requires the storage of the matrices gener-

ated in the steps of the infinite size system (fig. 3.3). The environment it is not builded from the system. Instead one utilizes the environments previously formed and stored by the infinite size algorithm.

The finite size system is implemented with the following algorithm:

1. perform the steps for the infinite size algorithm to form a superblock of size L but storing the matrix operators for the system and environment at each iteration.
2. Take the system block of size l from previous calculations and perform steps 2 to 7 for the infinite size algorithm to obtain a new system block of size $l + 1$ (the first iteration begins with $l = \frac{L}{2} - 1$). Store the $l + 1$ -system block replacing the old system of the same size stored (if no old system is, just store it).
3. Form a superblock of size L with the system block (l), two single sites (2) and the environment block ($l' = L - l - 2$). The environment is taken from the immediately last calculation for such environmet block size (from infinite or finite algorithm).
4. Perform steps 2 to 3 until $l = L - 3$ (i.e. $l' = 1$). This is the left to right sweep where the left block is enlarged.
5. Perform steps 2 to 3 reversing the roles of system and environmet blocks (interchange l by l'), i.e. switch direction of grow to enlarge the environment block.
6. Perform step 5 until $l' = 1$. This is the right to left sweep where the right block is enlarged.
7. Repeat starting with step 2 until convergence is reached.

The goal of the finite size algorithm is to maintain a fixed size for the super block by using complementary system and environment blocks. The size of the environment goes from edge to edge so it behaves as a zipper. In doing the

3.1. Basics on DMRG

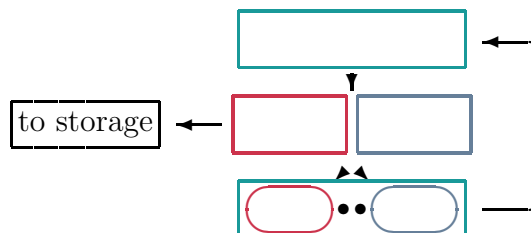


Figure 3.3: *The steps for the infinite size algorithm are performed until the superblock reaches the desired size while at each step the matrices for the system and the environment are stored. These matrices are used by the finite size algorithm to construct the super block utilizing complementary system and environment blocks.*

steps two sites in a complete basis are included in the superblock so after a number of iterations it resembles the superblock in an exact basis.

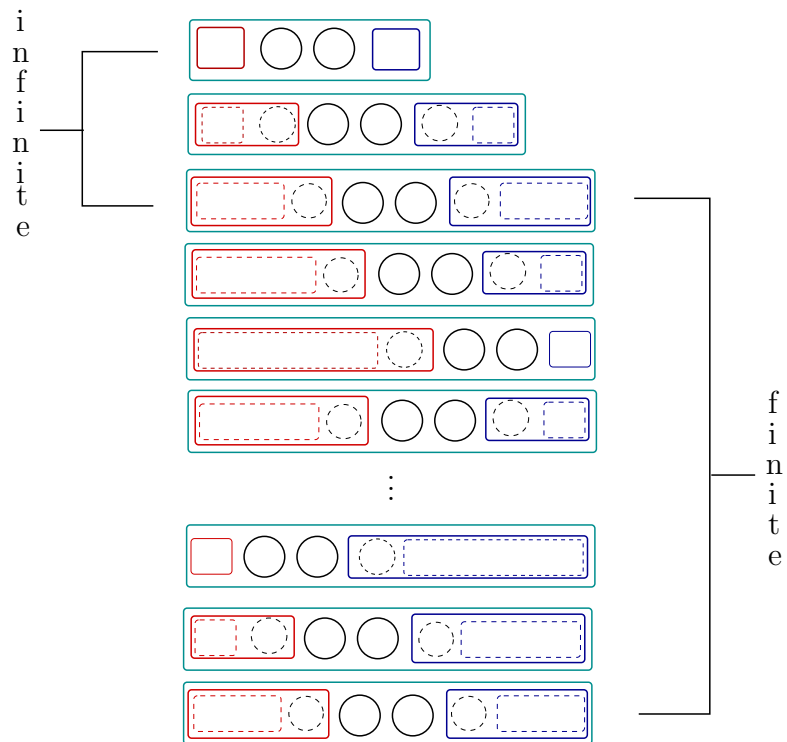


Figure 3.4: *The finite system start with a super block builded from the infinite size algorithm and then it uses the matrices formed in the infinite size algorithm to construct superblock of a fixed size.*

3.2 Description of the method

In this section we describe the DMRG method. Here we explain how the operators are worked out such that we can manage the dimension of the Hilbert space of the involved blocks. For this propose we consider two state particles forming the blocks.

We start the description with a L -sites superblock and then perform the DMRG steps ³ until a superblock of $L + 2$ sites is reached. The iterative nature of the method allow us understand the whole mechanism of the management of the Hilbert space with these few steps

3.2.1 Management of Hilbert space

Consider a one-diemnsional system of L sites as is shown in fig. 3.5.



Figure 3.5: *A system of L sites. It can be viewed as composed by two identical blocks.*

Split this system into two parts, both with $l = \frac{L}{2}$ sites and let us call to the first half as the system block and to the second one as the environmet block as is used in DMRG⁴.

We can notice that the dimension of the Hilbert space of each block is 2^l .

We denote by $|\varepsilon_k\rangle$ the basis of the Hilbert space corresponding to the k -th site of the block system with $k = 1, 2, \dots, L$ expand the Hilbert space of the k -th site in the system block. The basis $\{|\uparrow\rangle, |\downarrow\rangle\}$ can be an example of this procedure (see fig. 3.6).

³This description can be for both the infinite size and the finite size algorithms

⁴Here we have assumed the step of adding a site to a previous system and environmet blocks as is stated in the algorithms.

3.2. Description of the method

Let $|i\rangle = |\varepsilon_1\rangle|\varepsilon_2\rangle \cdots |\varepsilon_l\rangle$ be a vector describing the state of the system block. The rest of the system, the environment block is identified by the ket $|j\rangle = |\varepsilon_{l+1}\rangle|\varepsilon_{l+2}\rangle \cdots |\varepsilon_L\rangle$.

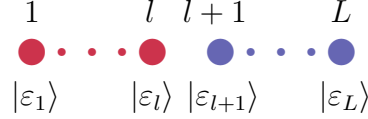


Figure 3.6: *The Hilbert space of the entire system is expanded by the tensorial product of each individual site state.*

The two block states, $|i\rangle$ and $|j\rangle$ are both 2^l -dimensional vector states. Then, the direct product $|i\rangle \otimes |j\rangle$ define a basis for the complete system that we call superblock (system + environment). Thus, the eigenvectors of the Hamiltonian of L sites can be expressed in terms of this basis. In particular the ground state can be expanded as,

$$|\Psi_0\rangle = \sum_{ij} \Psi_{ij} |i\rangle |j\rangle \quad (3.8)$$

where $\Psi_{ij} = \langle i | \langle j | \Psi_0 \rangle$. Here $|i\rangle |j\rangle$ is a set of $2^l \times 2^l = 2^{2l} = 2^L$ vectors.

Now, we can construct the reduced density matrix ρ for the system block. The matrix elements of ρ are given as follows

$$\rho_{ii'} = \sum_j \Psi_{ij}^* \Psi_{i'j} \quad (3.9)$$

Notice that ρ is a $2^l \times 2^l$ square matrix because $i, i' = 1 \dots 2^l$. After diagonalizing ρ , we can arrange the set of eigenvectors in a matrix, say O , where the columns are the eigenvectors arranged from the largest one to the lowest one. Again, O is a $2^l \times 2^l$ square matrix. If we take only the m largest eigenvectors, thus O becomes a $2^l \times m$ matrix.

Let us construct the system block Hamiltonian H_S and change the basis to the m selected eigenvectors of the density matrix. Thus, we obtain a transformed

Hamiltonian \tilde{H}_S :

$$\begin{aligned}\tilde{H}_S &= O^\dagger(m \times 2^l)H_S(2^l \times 2^l)O(2^l \times m) \\ &= \tilde{H}_S(m \times m)\end{aligned}\tag{3.10}$$

We apply the same unitary transformation to any operator of interest from the subsystems and then every such operator becomes a $m \times m$ matrix (with $m \leq 2^l$). With this we have transformed any relevant operator from the subsystems to an optimal basis for the system block, whenever we can use reflection symmetry. Otherwise we will need to construct additionally the reduced density matrix for the environment block.

Now we add an extra site to the right of the system and an extra site to the left of the environment as shown in fig. 3.7.

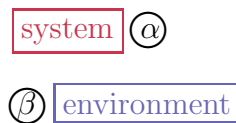


Figure 3.7: *Two new sites has been added to the original superblock, labeled α and β .*

A superblock of size $L + 2$ can be formed as shown in fig. 3.8. The base of

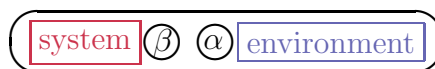


Figure 3.8: *The dashed rectangles are the system and the environment formed in the current iteration. A site is added to each one to form the corresponding system an environment for following iterations.*

this new superblock is of the form:

3.2. Description of the method

$$|\tilde{i}\rangle|\alpha\rangle|\beta\rangle|\tilde{j}\rangle \quad (3.11)$$

where $|\tilde{i}\rangle$ and $|\tilde{j}\rangle$ are the eigenvectors of the density matrix and $|\alpha\rangle$ and $|\beta\rangle$ are the base of the sites α and β respectively ⁵. Here, $|\tilde{i}\rangle$ and $|\tilde{j}\rangle$ are associated to the system and the environment respectively and $|\alpha\rangle$ and $|\beta\rangle$ to the extra sites. Noting that $|\tilde{i}\rangle$ and $|\tilde{j}\rangle$ are sets of m vectors and $|\alpha\rangle$ and $|\beta\rangle$ are two state sets, for the superblock we have a set of $2m \times 2m$ vectors.

In terms of this basis, any vector describing the state of the superblock can be expressed as follows:

$$|\tilde{\Psi}\rangle = \sum_{\tilde{i}\alpha\beta\tilde{j}} \Psi_{\tilde{i}\alpha\beta\tilde{j}} |\tilde{i}\rangle|\alpha\rangle|\beta\rangle|\tilde{j}\rangle. \quad (3.12)$$

Then we proceed as in the previous steps, by using this superblock as the new input for the renormalization step. Again we divide the superblock in two subsystems that we call system and environment, but now each one has one site more than the previous subsystems as is shown in fig. 3.9.

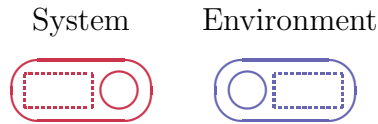


Figure 3.9: *The system and the environment blocks consists of a block in a truncated basis plus one site in an exact basis.*

Let us make the following relabeling of the states:

$$\begin{aligned} |\tilde{i}\rangle|\alpha\rangle &\rightarrow |l\rangle, \\ |\tilde{j}\rangle|\beta\rangle &\rightarrow |r\rangle. \end{aligned} \quad (3.13)$$

⁵Note that for α and β the basis is exact.

Thus, the label l refers to the system and r to the environment. Then,

$$\rho_W = \sum_r \Psi_{l_r}^* \Psi_{l_r} \quad (3.14)$$

is the reduced density matrix of the system block. Thus, because there are $2m$ vectors for the system block (the set $\{|l\rangle\}$ consisting of $2m$ states), then ρ_W is a $2m \times 2m$ matrix.

Now we can construct the transformation matrices and more over we can transform the system and the environment blocks by means of the matrices O and O^\dagger as discussed previously. Because the later matrices are $2m \times m$ and $m \times 2m$ respectively, the transformed operators are again $m \times m$ matrices.

Chapter 4

The Hubbard model

4.1 Some aspects of the Hubbard model

In the following we will make use of second quantization operators and the model Hamiltonian we will refer is the known as Hubbard Model which is usually expressed in terms of these operators.

Let us start by considering a simple case, namely a single hydrogen atom. We know that one hydrogen atom has only one electron, in the so called s-orbital. This electron can be in either a spin-up or spin-down state. This given orbital (s-orbital) can be occupied by at most two electrons, one-up and one-down. We have also learned that a real hydrogen atom also has many other orbitals where the electrons can go, but we will consider only this single orbital. Now, let us assume we have an array of hydrogen atoms, each one is connected to two others (if we consider a one-dimensional topology). In this chain, due to some processes, the electrons are allowed to hop from site to site, mainly from one to the next site but considering a symmetric hopping from a given site i . This approximation is also called tight-binding approximation.

Now let us go a little bit further and include several electrons in the lineal chain. We know that electrons are negatively charged particles, and like charges repel. We would like to consider this repulsion in our model. This repulsion is very long tailed by $1/r$ behavior, where r is the distance between two given electrons.

Due to the discrete nature of our approximations here we should try to include the repulsion in a discrete manner. Perhaps the crudest approximation can be described as follows:

- Two electrons do not interact with each other, if they do not are located within the same hydrogen atom.
- The strength of the Coulombic repulsion is given by U and it is different of zero only when the electrons are at the same site.
- The electrons located at the same site have opposite spins following Pauli exclusion principle.

This approximation to the repulsion is also called the *on-site repulsion*. With this respective term and with the hopping part we are able to model the movement of electrons on a periodic lattice. They are the main ingredients of the *Hubbard model*.

It is important to mention that the Hubbard model is not restricted to the on-site repulsion or to a single orbital, but this is the situation defining the model. In any case, here we focus in the simplest version just noticing that the methods we describe here can be easily extrapolated to more complicated cases. The model is then summarized by the parameters, the energy gain t due to hopping of the electrons between nearest neighbor sites, which in effect represents the kinetic energy, and the energy cost U to have two electrons at the same site, which is the dominant contribution to the Coulomb energy.

In what follows we shall mean the Hubbard model the one-dimensional one-band electronic model with nearest-neighbor hopping as defined by the Hamiltonian [10]

$$H = -t \sum_{j=1}^L \sum_{a=\uparrow,\downarrow} (c_{j,a}^\dagger c_{j+1,a} + c_{j+1,a}^\dagger c_{j,a}) + U \sum_{j=1}^L n_{j\uparrow} n_{j\downarrow}. \quad (4.1)$$

Here $c_{j,a}^\dagger$ and $c_{j,a}$ are creation and annihilation operators respectively of electrons of spin a ($a = \uparrow$ or \downarrow) localized within an orbital at site j of a one-dimensional lattice, and $n_{j,a} = c_{j,a}^\dagger c_{j,a}$. The parameters U and t are real numbers, setting

4.1. Some aspects of the Hubbard model



Figure 4.1: A valid configuration for a Hubbard chain. The contribution to the coulomb energy is $2U$

the energy scale and the relative strength of the two sums that contribute to the Hamiltonian [10].

The operators $c_{j,a}^\dagger$ and $c_{j,a}$ are Fermi operators. They satisfy the anticommutation relations

$$\begin{aligned} \{c_{j\alpha}, c_{k\beta}\} &= \{c_{j\alpha}^\dagger, c_{k\beta}^\dagger\} = 0, \\ \{c_{j\alpha}, c_{k\beta}^\dagger\} &= \delta_{jk}\delta_{\alpha\beta} \end{aligned} \quad (4.2)$$

for $j, k = 1, \dots, L$ and $a, b = \uparrow, \downarrow$. The creation operators $c_{j,a}^\dagger$ generate the space of states of the Hubbard model by acting on the vacuum state $|0\rangle$ defined by the condition

$$c_{j,a}|0\rangle = 0, \quad j = 1, \dots, L, \quad a = \uparrow, \downarrow. \quad (4.3)$$

The states of the model are given by specifying the four possible configurations of each site on a lattice made of L sites. Each site can either be empty, contain one electron with either of the two spins, or two electrons of opposite spins. Thus, the basis used for the sites is $\{|\downarrow\rangle, |0\rangle, |\downarrow\uparrow\rangle, |\uparrow\rangle\}$. The hopping term alone leads to a conventional band spectrum and one-electron Bloch levels in which electronic wavefunction is distributed throughout the entire crystal (a metal). The interaction term (also called Coulomb term) if taken alone, would favor local magnetic moments, since it suppress the possibility of a second electron (with oppositely directed spin) at a singly occupied sites (an insulator). When both terms are present, the competition between them brings about a transition between the metallic phase and the Mott insulating phase [19].

The Hubbard model, as we can see, is characterized through the parameters t, U of the Hubbard Hamiltonian and through the so called *filling factor* given by:

$$f = \frac{N}{N_0}, \quad (4.4)$$

where N is the electron number and N_0 is the number of sites. The filling factor f can take values within $0 \leq f \leq 2$. The case $f = 1$ is termed the *half filling* case.

The Hubbard model was exactly solved by means of the Bethe ansatz by Lieb and Wu [20] and the ground state energy for the half-filled case with $S^z = 0$ can be expressed in the form

$$E_0 = -4Nt \int_0^\infty \frac{dx}{x} J_0(x) J_1(x) f(xU/2t) \quad (4.5)$$

where J_0 and J_1 are Bessel functions of zero and first order respectively and $f(z) = [1 + e^z]^{-1}$ [26].

4.2 The one-dimensional Hubbard model and experiments

The one-dimensional Hubbard model has been of great conceptual value in facilitating the interpretation of experiments on quasi one-dimensional materials. Although it is not strictly a perfect model for any existing material, many of its qualitative features seem to be realized in nature. At present there is a sizeable list of materials, for which the electronic degrees of freedom are believed to be described by "Hubbard-like" Hamiltonians. Examples are the chain cuprates Sr_2CuO_3 and $SrCuO_2$, organic conductors such as the Bechgaard salts or TTF-TCNQ and π -conjugated polymers like polydiacetylene¹.

¹Taken from The One-dimensional Hubbard model [10].

4.3 Symmetries in the Hubbard model

There are some basic symmetries of the Hubbard model which should well understood and used as a foundation on which to build more understanding. They may be exploited to reduce storage and computation time and to thin out Hilbert space by decomposing it into a sum of sectors. The particle total number operator

$$N = \sum_j^L (n_{j,\uparrow} + n_{j,\downarrow}), \quad (4.6)$$

commutes with the Hamiltonian and hence is conserved. The electron density is therefore a good quantum number and calculations at different densities are effectively independent of each other. The total spin

$$S^z = \frac{1}{2} \sum_j^L (n_{j,\uparrow} - n_{j,\downarrow}) \quad (4.7)$$

is also conserved and so states with different ferromagnetic moments are decoupled [8]. These two symmetries are resumed in the commutation relations

$$[H, N] = 0 \quad (4.8)$$

and

$$[H, S^z] = 0 \quad (4.9)$$

In diagonalizing the Hamiltonian it is useful to classify the basis states by quantum numbers, since the Hamiltonian is block diagonal. The structure of the operators that commute with the Hamiltonian is of the form, for a single site

$$\begin{array}{c}
| \downarrow \rangle \\
| 0 \rangle \\
| \downarrow \uparrow \rangle \\
| \uparrow \rangle
\end{array}
\begin{array}{c}
| \downarrow \rangle \\
| 0 \rangle \\
| \downarrow \uparrow \rangle \\
| \uparrow \rangle
\end{array}
\begin{bmatrix}
H_{\downarrow} & & & \\
& H_0 & & \\
& & H_{\downarrow \uparrow} & \\
& & & H_{\uparrow}
\end{bmatrix}
\quad (4.10)$$

where, for instance H_{\downarrow} is spanned by all the vectors corresponding to charge 1 and S^z equal to -1 in which case there is only one vector, $| \downarrow \rangle$. Consequently H_{\downarrow} is a 1×1 matrix, i.e. a scalar.

The structure of these matrices is called block-diagonal because the non-zero entries are arranged in blocks along the principal diagonal. With the basis arranged in the same order, we can write the the basic operators in matrix form as follows:

$$c_{\downarrow}^{\dagger} = \begin{pmatrix} 0 & 1 & 0 & 0 \\ 0 & 0 & 0 & 0 \\ 0 & 0 & 0 & 1 \\ 0 & 0 & 0 & 0 \end{pmatrix} \quad (4.11)$$

$$c_{\uparrow}^{\dagger} = \begin{pmatrix} 0 & 0 & 0 & 0 \\ 0 & 0 & 0 & 0 \\ -1 & 0 & 0 & 0 \\ 0 & 1 & 0 & 0 \end{pmatrix} \quad (4.12)$$

$$n_{\uparrow} = \begin{pmatrix} 0 & 0 & 0 & 0 \\ 0 & 0 & 0 & 0 \\ 0 & 0 & 1 & 0 \\ 0 & 0 & 0 & 1 \end{pmatrix} \quad (4.13)$$

4.4. Composite systems for the Hubbard model

$$n_{\downarrow} = \begin{pmatrix} 1 & 0 & 0 & 0 \\ 0 & 0 & 0 & 0 \\ 0 & 0 & 1 & 0 \\ 0 & 0 & 0 & 0 \end{pmatrix} \quad (4.14)$$

and

$$\Omega = n_{\uparrow} n_{\downarrow} = \begin{pmatrix} 0 & 0 & 0 & 0 \\ 0 & 0 & 0 & 0 \\ 0 & 0 & 1 & 0 \\ 0 & 0 & 0 & 0 \end{pmatrix} \quad (4.15)$$

4.4 Composite systems for the Hubbard model

In the following, we set $t = U = 1$. To express the above operators in a basis for two or more sites we make usage of the tensor product. For two sites, we have

$$H_{2\text{-sites}} = \sum_{\sigma} (c_{1\sigma}^{\dagger} \cdot c_{2\sigma} + H.c.) + \Omega_1 + \Omega_2 \quad (4.16)$$

For the first particle we can write:

$$c_{1\sigma}^{\dagger} = c_{\sigma}^{\dagger} \otimes I \quad (4.17)$$

$$\Omega_1 = \Omega \otimes I \quad (4.18)$$

and for the second-one:

$$c_{2\sigma}^{\dagger} = I \otimes c_{\sigma}^{\dagger} \quad (4.19)$$

$$\Omega_2 = I \otimes \Omega, \quad (4.20)$$

where I is the 4×4 identity matrix and $c_{1\sigma}$ and $c_{2\sigma}$ are obtained as the Hermitian of eqs. (4.17) and (4.19) respectively. Then, the Hamiltonian for two sites will be

$$\begin{aligned}
H_{2\text{-sites}} &= \sum_{\sigma} [(c_{\sigma}^{\dagger} \otimes I) \cdot (I \otimes c_{\sigma}) + H.c.] \\
&+ \Omega \otimes I + I \otimes \Omega
\end{aligned} \tag{4.21}$$

that can be rewritten as

$$H_{2\text{-sites}} = \sum_{\sigma} (c_{\sigma}^{\dagger} \otimes c_{\sigma} + H.c.) + \Omega \otimes I + I \otimes \Omega, \tag{4.22}$$

because of the identity $(A \otimes B) \cdot (C \otimes D) = A \cdot C \otimes B \cdot D$.

If we add one more site, then the involved operators are:

- for the first site

$$c_{1\sigma}^{\dagger} = c_{\sigma}^{\dagger} \otimes I^{\otimes 2} \tag{4.23}$$

$$\Omega_1 = \Omega \otimes I^{\otimes 2} \tag{4.24}$$

- for the second

$$c_{2\sigma}^{\dagger} = I \otimes c_{\sigma}^{\dagger} \otimes I \tag{4.25}$$

$$\Omega_2 = I \otimes \Omega \otimes I \tag{4.26}$$

- and for the third

$$c_{3\sigma}^{\dagger} = I^{\otimes 2} \otimes c_{\sigma}^{\dagger} \tag{4.27}$$

$$\Omega_3 = I^{\otimes 2} \otimes \Omega. \tag{4.28}$$

Here the notation $I^{\otimes 2}$ means $I \otimes I$.

Let us consider the four sites Hamiltonian, which in the above notation is written as:

4.4. Composite systems for the Hubbard model

$$\begin{aligned}
H_{4\text{-sites}} &= \sum_{\sigma} (c_{\sigma}^{\dagger} \otimes c_{\sigma} \otimes I^{\otimes 2} + H.c.) + (\Omega \otimes I) \otimes I^{\otimes 2} + (I \otimes \Omega) \otimes I^{\otimes 2} \\
&+ \sum_{\sigma} (I \otimes c_{\sigma}^{\dagger} \otimes c_{\sigma} \otimes I + H.c.) \\
&+ \sum_{\sigma} (I^{\otimes 2} \otimes c_{\sigma}^{\dagger} \otimes c_{\sigma} + H.c.) + I^{\otimes 2} \otimes (\Omega \otimes I) + I^{\otimes 2} \otimes (I \otimes \Omega),
\end{aligned} \tag{4.29}$$

or equivalently the Hamiltonian for a four-sites system can be written as

$$\begin{aligned}
H_{4\text{-sites}} &= H_2^L \otimes I^{\otimes 2} \\
&+ (c_{rm}^{\dagger} \otimes c_{lm} + H.c.) \\
&+ I^{\otimes 2} \otimes H_2^R
\end{aligned} \tag{4.30}$$

where H_2^L and H_2^R are both given by eq. (4.22) and

$$c_{rm}^{\dagger} = I \otimes c_{\sigma}^{\dagger} \tag{4.31}$$

$$c_{lm} = c_{\sigma} \otimes I \tag{4.32}$$

In eq. (4.30), the operator H_2^L concerns with the first two sites and H_2^R with the last two sites from left to right as is shown in fig. 4.2.

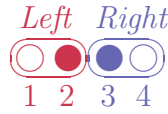


Figure 4.2: *Sites 1 and 2 correspond to the Left side subsystem and 3 and 4 to the Right side subsystem. The sites in contact between the subsystems are the right most of the Left subsystem (site 2) and the left most for the Right subsystem (site 3).*

The subscripts rm and lm in eqs. (4.30) and (4.31) and (4.32) refer respectively to the *right most* site of the *Left* subsystem and to the *left most* site from the *Right* subsystem, and then c_{rm}^{\dagger} and c_{lm} are respectively the operators for the sites 2 and 3 (see fig. 4.2). Thus, this allows to express a Hamiltonian in terms of Hamiltonians of less sites than the original.

4.5 DMRG for the Hubbard chain

The basis of a four-site superblock is the tensor product of the bases of each one of the sites:

$$\begin{pmatrix} |\downarrow\rangle \\ |0\rangle \\ |\downarrow\uparrow\rangle \\ |\uparrow\rangle \end{pmatrix} \otimes \begin{pmatrix} |\downarrow\rangle \\ |0\rangle \\ |\downarrow\uparrow\rangle \\ |\uparrow\rangle \end{pmatrix} \otimes \begin{pmatrix} |\downarrow\rangle \\ |0\rangle \\ |\downarrow\uparrow\rangle \\ |\uparrow\rangle \end{pmatrix} \otimes \begin{pmatrix} |\downarrow\rangle \\ |0\rangle \\ |\downarrow\uparrow\rangle \\ |\uparrow\rangle \end{pmatrix}, \quad (4.33)$$

which generates a Hilbert space basis of $4^4 = 256$ orthogonal states. We can take advantage of the symmetry of the model and fix the charge and the z component of the total spin. For instance, if we fix $S_z = -1$ and $N_e = 1$ we only need to work within this specific sector of Hilbert space, i.e., with the basis $\{|\downarrow, 0, 0, 0\rangle, |0, \downarrow, 0, 0\rangle, |0, 0, \downarrow, 0\rangle, |0, 0, 0, \downarrow\rangle\}$.

Now we split the system into two parts, each of two sites like in fig. 4.2. Suppose we have diagonalized this system and found its ground state $|\Psi_0\rangle$. Then we can find ρ and the transformation matrices O and O^\dagger . Now, from eq. (3.8) we can see that ρ is a 3×3 matrix. Therefore, O can at most be a 3×3 matrix, and the same holds for O^\dagger . Applying the definition given by (3.8) we have that:

$$\rho = \begin{pmatrix} \rho_{(\downarrow,0)(\downarrow,0)} & \rho_{(\downarrow,0)(0,\downarrow)} & \rho_{(\downarrow,0)(0,0)} \\ \rho_{(0,\downarrow)(\downarrow,0)} & \rho_{(0,\downarrow)(0,\downarrow)} & \rho_{(0,\downarrow)(0,0)} \\ \rho_{(0,0)(\downarrow,0)} & \rho_{(0,0)(0,\downarrow)} & \rho_{(0,0)(0,0)} \end{pmatrix}, \quad (4.34)$$

where for example $\rho_{(\downarrow,0)(0,\downarrow)}$ refer to the coefficients of the vectors of the form $|\downarrow, 0 \dots\rangle$ and $|0, \downarrow \dots\rangle$ and of course, the entries of this matrix are summation as is stated by eq. (3.8).

4.6 Results

To test our DMRG implementation we present some results for the one dimensional Hubbard model and compare with other analytical and numerical tech-

4.6. Results

niques, even DMRG calculations performed by other authors [22] [21]. Here, we provide some calculations focused on the half filling case and compare to the published results from [21]. Our implementation works for even and odd size chains but for comparison with the exact result given by eq. (4.5) we consider a 16-site chain at half filling and total S^z component value 0. Also, we show results for some arbitrary fillings and give a brief discussion about.

4.6.1 Discussion

We use the DMRG technique to calculate the ground state energy for a 16-site chain in the framework of the Hubbard model at half-filling with $S^z = 0$. The results are given in table 4.1 for $U = 0$ (non-interacting case) and several sizes maintaining up to 100 states. They are compared to the exact energy obtained by eq. (4.5) and with the results of a similar Thesis on DMRG by Dan Bohr at the Technical University of Denmark [22].

It can be noticed that our results have a slightly improvement with respect to the work of Bohr, but this can be attributed to the fact that he takes up to 25 eigenstates of the reduced density matrix while we go a little bit upper here.

The behavior for fixed size, as U goes from 0 to the highest values is shown in fig. 4.3 for exact and DMRG calculations. For large U the system tends to be in a single occupied sites state because of the high energy cost of double occupation, while for lower U the competition between kinetic and potential energy gives the characteristic curve showed in fig. 4.3. In the limit of $U \rightarrow 0$, all spin configurations are possible and the electrons move freely through the sites of the chain. In addition, it is shown a plot of the difference of both calculations as a function of U . It can be noticed that the difference decreases as U increases.

In fig. 4.4 we show the ground state energy per site for several chain sizes ranging from 20 to 90 sites with $U/t = 1$. Notice the convergence to the exact value for the energy per site ~ -1.04 . In table 4.2 we compare the convergence to exact ground state energy per site within different values of m . For other than

L	Exact (from ref [20])	DMRG finite-size (present work)	DMRG finite size (from ref [22])
8	-10.185916	-9.517540	
10	-12.732395	-12.05334	
12	-15.278874	-14.59245	-14.5895
14	-17.825353	-17.13354	
16	-20.371832	-19.67588	
18	-22.918311	-22.21910	
20	-25.464790	-24.76292	-24.7183

Table 4.1: *Comparison of the ground state energy for the Hubbard model obtained from eq. (4.5) and the obtained by DMRG for a 16 sites chain at half filling and $S_z = 0$.*

m	DMRG (present work)	DMRG (Momentum space [21])
10	-0.986664	
50	-0.999592	
100	-0.999621	
400		-1.02925
1000		-1.02958

Table 4.2: *Comparison of our results with a low number of retained states with those obtained by DMRG in momentum space in [21].*

4.6. Results

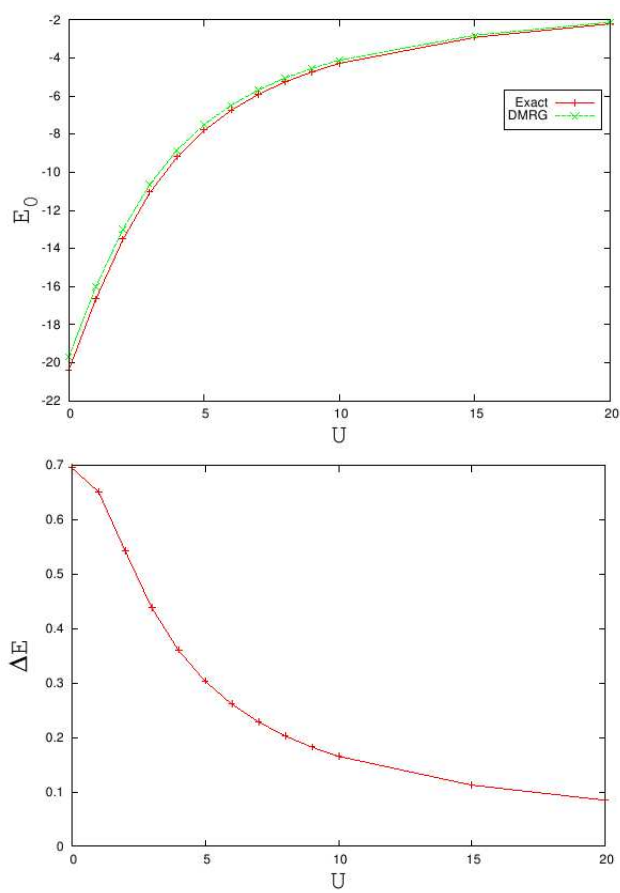


Figure 4.3: Energy from DMRG and Bethe Ansatz for the ground state with $t=0$ and the difference between them ΔE as a function of the U parameter.

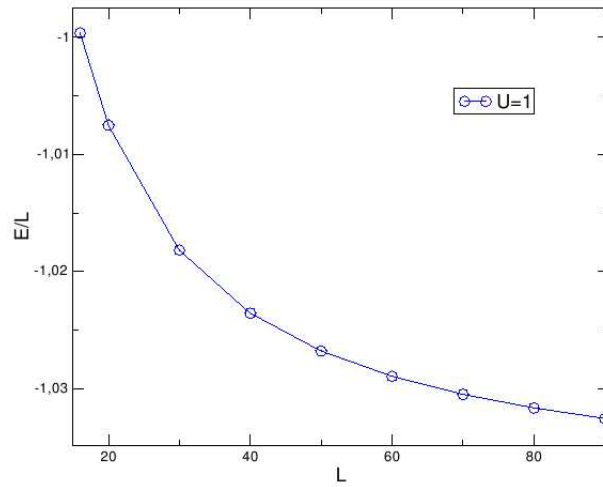


Figure 4.4: *Energy per site as a function of the number of sites with $U = 1$.*

the half filling case, results are showed in figs. 4.5 and 4.6. Figure (4.5) shows some plots for the energy as a function of the number of particles (electrons) for $U/t = 0$ through 9. When $U = 0$ (noninteracting electrons) only the hopping contribution is present, so the electrons can flow through the sites with no other restriction than double occupancy. A minimum in the energy is founded at half filling ($N = 16$), and the energy is symmetric around it. This perhaps is because in the noninteracting case the number of moving electrons is symmetric respect to half filling. For other values of U/t we can see a minimum for the energy and a discontinuity point. The minimum goes to lower number of electrons as U/t increases and the discontinuity point is maintained at $N = 16$. We can see from fig. 4.5 that as the number of particles is increased, the U contribution becomes more important. Beyond the energy minimum the U contribution dominates slowly and after the discontinuity point it happen drastically. This is because beyond half filling, on site energy grows almost linearly with double occupancy and hopping term could vanish.

The behavior can also be observed in fig. 4.6 in which we plot the curves for the energy as a function of U/t fixing $t = 1$ ranging from 2 to 20 electrons in a 16-sites chain. For electron configurations below half filling, the energy reaches a

4.6. Results

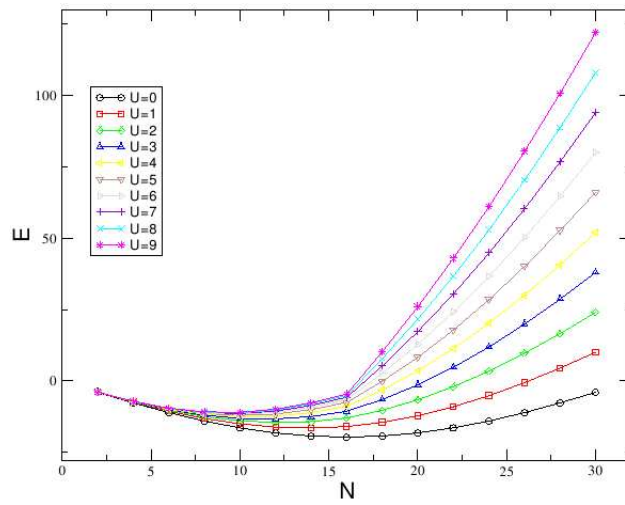


Figure 4.5: *Plot of the ground state energy as a function of the number of electrons in a 16-sites chain*

convergence limit for $U = \infty$. Such a configuration avoid double occupancy. For above half filling, it is impossible to avoid double occupancy and so the energy increases when U is increased giving a behavior almost linear as one can see for 18 and 20 electrons in fig. 4.6.

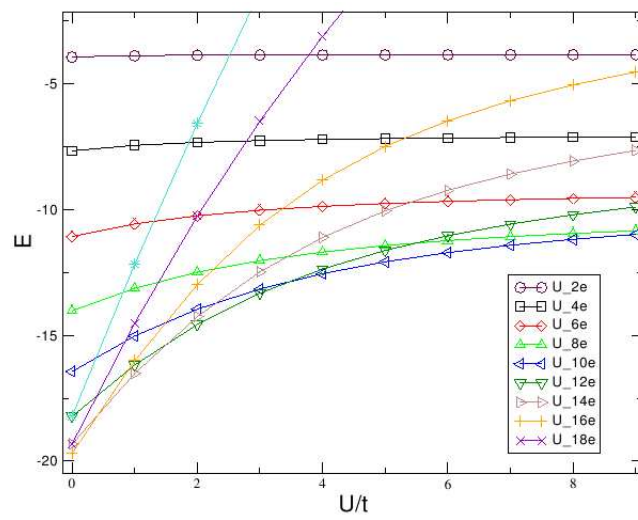


Figure 4.6: Plots of the ground state energy as a function of U/t for a 16 sites chain varying the number of electrons from 2 to 18.

Chapter 5

An electron-phonon interaction Hamiltonian

Here we are interested in applying the power of the Density Matrix Renormalization Group method to describe a model Hamiltonian studied until now for a 3-sites inhomogeneous linear cuprate system, consisting of two oxygen atoms surrounding a Cu atom [29–34]. Such cluster gives superconductivity behavior to the $\text{YBa}_2\text{Cu}_3\text{O}_{7-\delta}$ ceramic superconductor. Phonons play a fundamental role in our understanding of sound, heat, elasticity and electrical resistivity in solids. More surprising may be the fact that the electron-phonon coupling appear to be the cause of conventional Superconductivity [9]. For this reason it is necessary to have the knowledge of how one may proceed when bosonic degrees of freedom are dealt. The simplest conceptual approach is to arbitrarily truncate the local state to a given finite number for the bosonic degrees of freedom, and to check for DMRG convergence. This approach has been very successful in the context of the Bose-Hubbard model where the on-site Coulomb repulsion U suppresses large occupation numbers. It has been used to obtain the phase diagram of the one-dimensional extended Bose-Hubbard model by using a small bosonic basis (4 to 5 boson states) [38]. Additionally, it has been used to discuss the nature of the different ground states of the half filled Holstein model of spinless fermions in 1D [39]. Other applications that are more problematic have been phonons, both

5.1. Large number of degrees of freedom

with and without coupling to magnetic or fermionic degrees of freedom. While they are believed to be reliable to give a generic picture of physical phenomena, for more rigorous studies more elaborated techniques are necessary.

5.1 Large number of degrees of freedom

Essentially three approaches have been undertaken to reduce the large number of states per site to a small number that can be manageable by DMRG.

Bursill [40] has proposed a so-called *four block approach* that is particularly suited to periodic boundary conditions and is a mixture of Wilson numerical renormalization group and DMRG ideas. Starting from 4 initial block of size 1 with M states (this may be a relatively large number of electronic and phononic degrees of freedom) forming a ring, one solves for the ground state of that M^4 state problem; density matrices are then formed to project out two blocks, and form a new block of double size with M^2 states, which are truncated down to M using the density matrix information. With 4 of these blocks, a new 4 block ring is built, leading to a doubling of system size at every step.

An approach more in the spirit of DMRG, the so called *local state reduction* (which we will refer to as Optimal phonon basis method), was introduced by Zhang et al. [24]. Assuming fermionic and a small number of bosonic degrees of freedom on each site, one of the sites is chosen as "big site" to which a further number of bare bosonic degrees of freedom is added. Within a DMRG formulation, a density matrix is formed for the big site to truncate the number of optimal degrees of freedom. This procedure is repeated through the lattice in the finite-system algorithm. The standard prediction algorithm, makes the calculation quite fast. Physical quantities are then extracted within the optimal phononic state space. As can be seen from fig. 18, merely keeping two or three optimal states, in which high-lying bare states have non-negligible weight, may be as efficient as keeping of the order of hundred bare states. This approach has allowed to demonstrate the strong effect of quantum lattice fluctuations in trans-polyacetylene. Combined

with Lanczos vector dynamics, very precise dynamical susceptibilities have been extracted for spin-boson models.

Jeckelmann and White have devised a further approach [23] where 2^n bosonic degrees of freedom are embodied by n *pseudo-sites*: writing the number of the bosonic degree of freedom as a binary number, the degree of freedom is encoded by empty and full fermionic pseudo-sites. Finite-system DMRG is then applied to the resulting Hamiltonian. They have been able to study polaronic self-trapping of electrons in the Holstein model for up to 128 phonon states and have located very precisely the metal-insulator transition in this model.

5.2 Anomalies in $\text{YBa}_2\text{Cu}_3\text{O}_{7-\delta}$

In this section, we make a brief introduction to a phenomena under active research since more than a decade concerning to one of the first high- T_c discovered superconductors, the cuprate $\text{YBa}_2\text{Cu}_3\text{O}_7$ ($T_c = 93\text{K}$). The $\text{YBa}_2\text{Cu}_3\text{O}_7$ contains two Cu-O planes separated by a plane of atoms of Y between each Cu-O plane. The critical temperature seems to be maintained under a replacement of the atoms Y or Ba. However, it shows a great sensibility under substitution of the Cu or O atoms. For this reason it is established that the electronic coupling occurs in the Cu-O planes [35].

Genzel et. al. [27], have studied from theoretical approaches as well as from experiment infrared reflectivity of sintered $\text{YBa}_2\text{Cu}_3\text{O}_{7-\delta}$ focusing in phonon eigenfrequencies, half-widths and oscillator strength [27]. They found very strong phonon signals in the c direction (along the z axis in fig. 5.1) from the experimental studies. They perform lattice dynamics calculations and compare them with experimental data, founding a discrepancy. The oscillator strengths of the experimentally observed phonons were all stronger than those from a lattice dynamics calculation, specially for the 155 cm^{-1} mode with a strength 15 times larger than that predicted by theory. This mode has been labeled as the Barium mode and by charge transfer arguments it can be described as a rigid motion of the $[\text{CuO}_3]$

5.2. Anomalies in $\text{YBa}_2\text{Cu}_3\text{O}_{7-\delta}$

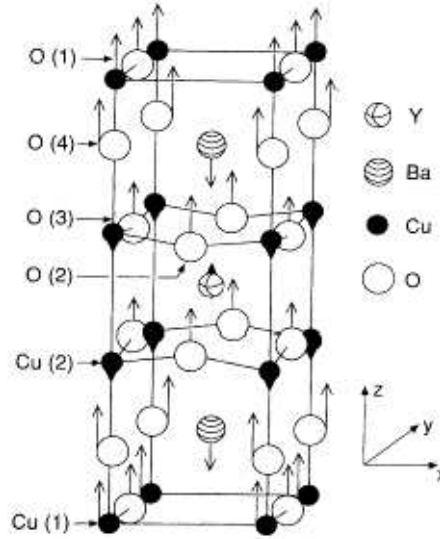


Figure 5.1: *Figure after [27] for $\text{YBa}_2\text{Cu}_3\text{O}_7$. Labels 1,2,3,4 are to identify such atom in such position.*

in one direction and Ba^{2+} ions in the opposite direction [27] (see fig. 5.1).

Using this ideas, Batistic et al. [28] propose a cluster model build on the suggestion of Genzel et al. [27] in which they take in count IR activity along c axis. Also, they consider the counterpart of the 155 mode, the Raman active mode corresponding to the symmetric oscillation of the O(4) ions within the cluster. The frequency assigned to this Raman mode is 515 cm^{-1} . Both modes can be described approximately by the asymmetric and symmetric oscillations, respectively of the O(4) oxygen atoms in the c direction [28].

XAFS data from $\text{YBa}_2\text{Cu}_3\text{O}_7$ have been presented which indicate that the O(4) atom moves in a double-well potential [30,31]. Mustre de León et al. propose an electron-phonon model Hamiltonian for describing the O(4)-Cu(1)-O(4) cluster in $\text{YBa}_2\text{Cu}_3\text{O}_7$ representing c -axis lattice electron coupling considering both infrared and Raman active vibrations [29].

This separation of the O(4)-Cu(1)-O(4) cluster from the rest of the lattice is valid because the dynamical coupling to the planes is weak due to the bond

lengths, and because some aspects of the coupling along the chain direction can be taken into account as an effective Hamiltonian by integrating out the degrees of freedom associated with the chain oxygen atoms O(1) [29].

The Hamiltonian proposed by Mustre de Leon et al. in [29] consists of an electronic part, a phononic part, and charge lattice interaction terms:

$$H = H_{el} + H_{el-ph} + H_{ph} \quad (5.1)$$

where

$$H_{el} = \sum_i \epsilon_i n_i + t \sum_{i\sigma} (c_{i\sigma}^\dagger c_{i\sigma} + H.c.) + U \sum_i n_{i\uparrow} n_{i\downarrow} \quad (5.2)$$

$$H_{ph} = \hbar\omega_{IR} b_{IR}^\dagger b_{IR} + \hbar\omega_R b_R^\dagger b_R \quad (5.3)$$

$$H_{el-ph} = -\lambda_{IR} (b_{IR} + b_{IR}^\dagger) (n_3 - n_1) - \lambda_R (b_R + b_R^\dagger) (n_1 - 2n_2 + n_3) \quad (5.4)$$

Here $n_{i\sigma} = c_{i\sigma}^\dagger c_{i\sigma}$ denotes the number operator for holes of spin σ at site i . Subscripts with $i = 1, 3$ refer to lower and upper O(4) sites, and $i = 2$ to the Cu(1) site, with site energies ϵ_i ($\epsilon_1 = \epsilon_3 = -\epsilon_2$), hopping amplitude t and on-site repulsion U . The phonon part of the Hamiltonian consists of harmonic Raman and infrared oscillators with creation operators b_R^\dagger and b_{IR}^\dagger and bare frequencies ω_R and ω_{IR} respectively. These operators are related to the Raman coordinate by $u_R = (\hbar/2m_O\omega_R)^{1/2} (b_R^\dagger + b_R) = (x_3 - x_1)/\sqrt{2}$, and to the infrared coordinate by

$$u_{IR} = \left(\frac{\hbar}{2m_O\omega_{IR}} \right)^{1/2} (b_{IR}^\dagger + b_{IR}) = \frac{x_1 + x_3 - (2m_O/m_{Cu})x_2}{(2 + 4m_O/m_{Cu})^{1/2}} \quad (5.5)$$

where x_1 and x_3 are the lower and upper O(4) coordinates respectively, and x_2 the Cu(1) coordinate measured from their equilibrium positions, and m_{Cu} and m_O are the Cu(1) and O(4) mass respectively.

The electron-phonon interaction term describes the favorable presence of Raman or infrared phonons whenever symmetric or antisymmetric charge distributions exist. For holes added at the Cu(1) site the Cu(1)-O(4) attraction is stronger leading to a short bond, while for holes added at the O(4) sites the attraction is

5.3. Generalization to a finite size chain

weaker, favoring a longer Cu(1)-O(4) bond length. For simplicity, only coupling between phonons and diagonal electronic terms is considered. The cluster has two phonon modes corresponding to displacements in the z direction (the cluster c-axis) that do not change the center of mass. These bare modes are assumed to be harmonic. They assume two holes within the O(4)-Cu(1)-O(4) cluster. In the ground state context, one hole is predominantly located at the Cu(1) site while the other fluctuates between the O(4) sites. This is in agreement with core level x-ray-absorption measurements implying excess holes located in the O(4) $2p_z$ orbitals [32].

5.3 Generalization to a finite size chain

Next, we describe the generalization used for the implementation of DMRG to an arbitrary odd number of sites to form a bigger chain. Here we do not propose a Hamiltonian which is accurately approached to the results presented by Mustre de León et al [29]. Rather a Hamiltonian in which interactions between vibrational modes and atomic sites are considered. The Hamiltonian is clearly separated in an electron-electron contribution, an electron-phonon contribution and a phonon-phonon part. In the electron-electron interaction, the terms corresponding to the repulsion and long range interaction are those given by a Hubbard Hamiltonian (see sec.(4.1)). The electronic part of the Hamiltonian is

$$H_{el} = \sum_i \epsilon_i n_i + t \sum_{i\sigma} (c_{i\sigma}^\dagger c_{i\sigma} + H.c.) + U \sum_i n_{i\uparrow} n_{i\downarrow}, \quad (5.6)$$

where the index i runs over all the sites of the oxygen and copper atoms and the interaction is to nearest neighbors. The involved operators are the familiar creation, annihilation and number operators for electronic states. The phonon Hamiltonian includes phonon-phonon interactions between phonon states from alternated sites as in the following Hamiltonian:

$$H_{ph} = \sum_{i,j} \hbar\omega_j b_{i,j}^\dagger b_{i,j} \quad (5.7)$$

where i indicates phononic sites and j runs over the normal modes of the system. The electron-phonon Hamiltonian is

$$H_{el-ph} = -\lambda_R \sum_i (b_{R,i}^\dagger + b_{R,i}) (n_{i-1} - 2n_i + n_{i+1}) - \lambda_{IR} \sum_{i'} (b_{IR,i'}^\dagger + b_{IR,i'}) (n_{i'+1} - n_{i'-1}) \quad (5.8)$$

The basis for a electronic site (a site without phonons) is $\{| \downarrow \rangle, |0\rangle, | \downarrow \uparrow \rangle, | \uparrow \rangle\}$ whereas the basis for a phononic site is the tensor product of the electronic basis with the phononic one:

$$\begin{pmatrix} | \downarrow \rangle \\ |0\rangle \\ | \downarrow \uparrow \rangle \\ | \uparrow \rangle \end{pmatrix} \otimes (|IR\rangle \otimes |R\rangle), \quad (5.9)$$

where $|IR\rangle$ is the basis for the infrared mode, whereas $|R\rangle$ correspond to the Raman mode.

5.4 Results

To have an idea of how the Raman and infrared states depend on the phonon number, we have calculated several energies ranging from 1 to 25 phonon (Raman and infrared) states. Then, we have chosen that corresponding to 3 Infrared and 8 Raman states. For the parameters in eq. (5.1) we use $\epsilon_{oxygen} = 0.5eV = -\epsilon_{copper}$, $t = -0.5eV$, and $U = 7.0eV$. For the bare phonon frequencies we use $\hbar\omega_R = 500cm^{-1} = 0.062eV$ and $\hbar\omega_{IR} = 612cm^{-1} = 0.076eV$. These are the same parameters used in the case of the O(4)-Cu(1)-O(4) cluster in [34].

The ground state energy shows a linear behavior with the increase of the number of sites whenever we maintain the electronic density and the total spin fixed. We fix the electronic density (charge/number of sites) and the spin number to 2/3 and 0 respectively, to calculate the energy as a function of the chain size. The results and the charge-size combinations are displayed in the table 4.1. Figure

5.4. Results

L	Q	Energy (eV)
9	6	-3.555130
15	10	-6.146724
21	14	-8.908199
27	18	-11.53220
33	22	-14.31081
39	26	-16.95529
45	30	-19.73647
51	34	-22.33522
57	38	-25.11881
63	42	-27.72379
69	46	-30.54633
75	50	-33.11992
81	54	-35.92911
87	58	-38.51736
93	62	-41.37423
99	66	-43.91807

Table 5.1: *The ground state energy for several sizes maintaining the ratio charge-size fixed to 2/3. L is the size and Q the charge corresponding to the energy E.*

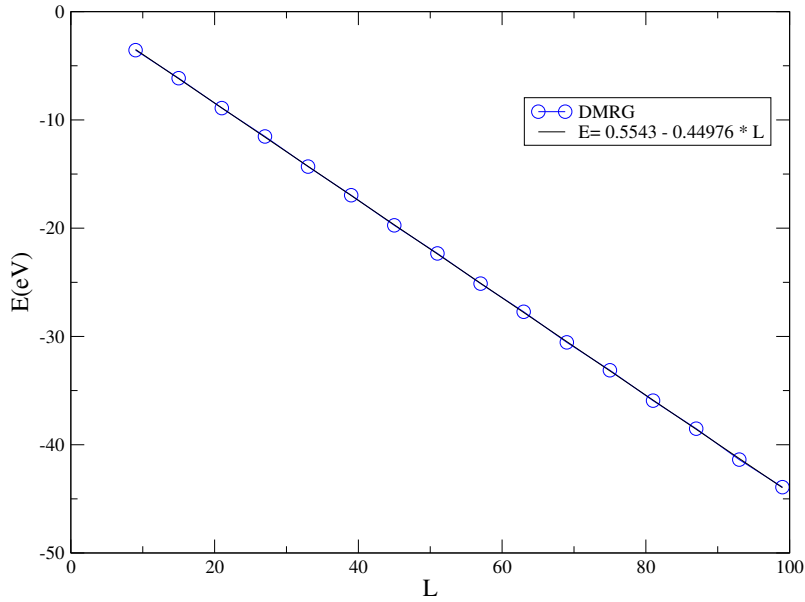


Figure 5.2: *The ground state energy plotted as a function of the number of sites.*

(5.2) shows the energy as a function of the number of sites.

For the three site chain, the ground state energy obtained by exact diagonalization is -0.67394 eV according to [36]. Performing a linear fit, we found that for the three sites chain the energy must be around -0.794 eV. We are expecting to obtain a value close to the exact because for three sites the Hilbert spaces coincide and the two Hamiltonians can be considered as the same. The difference of this value is almost 15% from the energy founded by Miranda [36].

5.5 The pseudosites approach

In this section the three-site cuprate system is analyzed in the framework of the pseudosite approach proposed by White and Jeckelmann [23]. Parameters are set according to [34] as in the previous section. First, a brief description of the method is given.

Boson degrees of freedom are in principle infinite, but in practice one needs to truncate to a finite number of boson states. Thus, in general we are dealing with a finite number of states labeled $\{|\alpha\rangle, \alpha = 0, 1, 2, \dots, M\}$. The pseudosite approach [23] allow to replace each boson state by one which correspond to a system of N pseudosites with a two-dimensional Hilbert space (see fig. 5.3). The idea is motivated by the representation of a number in binary form. In this case the number is a given boson state index α , starting with $\alpha = 0$. Each binary digit is represented by a pseudosite, which can be occupied (1) or empty (0). To

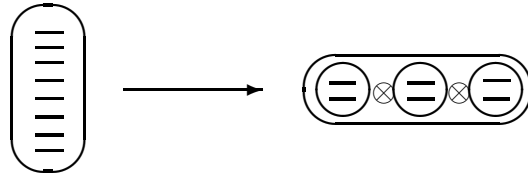


Figure 5.3: *Each Boson state is substituted by a state of a system of pseudosites.*

implement this idea, we first choose a truncated occupation-number basis of the form $\{|\alpha\rangle, \alpha = 0, 1, 2, \dots, M = 2^N - 1\}$, where $b^\dagger b|\alpha\rangle = \alpha|\alpha\rangle$; this will help to construct a finite Hilbert space of a boson site. Then we introduce N pseudosites $j = 1, \dots, N$, with a two dimensional Hilbert space $\{|r_j\rangle, r_j = 0, 1\}$ and operators a_j^\dagger, a_j such that $a_j|1\rangle = |0\rangle$, $a_j|0\rangle = 0$, and a_j^\dagger is the Hermitian conjugate of a_j . The one-to-one mapping between a boson level $|\alpha\rangle$ and the N -pseudosite state $|r_1 r_2 \dots r_N\rangle$ is given by the relation

$$\alpha = \sum_{j=1}^N 2^{j-1} r_j. \quad (5.10)$$

For instance, if we have only four boson states, namely $|0\rangle, |1\rangle, |2\rangle, |3\rangle$ so $M = 4$, then we need two pseudosites with states $|r_1 r_2\rangle$ because $N = 2$. Explicitly we are

doing the mapping

$$|0\rangle \Rightarrow |00\rangle$$

$$|1\rangle \Rightarrow |10\rangle$$

$$|2\rangle \Rightarrow |01\rangle$$

$$|3\rangle \Rightarrow |11\rangle$$

Next, we write all boson operators in terms of pseudosite operators. The boson number operator is given by

$$N_b = b^\dagger b = \sum_{j=1}^N 2^{j-1} a_j^\dagger a_j. \quad (5.11)$$

which can be easily checked. Then, if we have the Hamiltonian

$$H = \hbar\omega(b^\dagger b) \quad (5.12)$$

which in the occupation-number representation with four states takes the form

$$H = \begin{array}{c} \langle 0| \\ \langle 1| \\ \langle 2| \\ \langle 3| \end{array} \begin{array}{c} |0\rangle \\ |1\rangle \\ |2\rangle \\ |3\rangle \end{array} \begin{bmatrix} 0 & 0 & 0 & 0 \\ 0 & \hbar\omega & 0 & 0 \\ 0 & 0 & 2\hbar\omega & 0 \\ 0 & 0 & 0 & 3\hbar\omega \end{bmatrix}, \quad (5.13)$$

we would transform this system into a two-site system with Hamiltonian

$$H = \hbar\omega(2^0 a_1^\dagger a_1 + 2^1 a_2^\dagger a_2). \quad (5.14)$$

The operators a_1^\dagger and a_2^\dagger in the pseudosite representation are

$$a_1^\dagger = \begin{array}{c} \langle 00| \\ \langle 10| \\ \langle 01| \\ \langle 11| \end{array} \begin{array}{c} |00\rangle \\ |10\rangle \\ |01\rangle \\ |11\rangle \end{array} \begin{bmatrix} 0 & 0 & 0 & 0 \\ 1 & 0 & 0 & 0 \\ 0 & 0 & 0 & 0 \\ 0 & 0 & 1 & 0 \end{bmatrix} \quad (5.15)$$

5.5. The pseudosites approach

and

$$a_2^\dagger = \begin{array}{c} \langle 00| \\ \langle 10| \\ \langle 01| \\ \langle 11| \end{array} \begin{array}{c} |00\rangle \\ |10\rangle \\ |01\rangle \\ |11\rangle \end{array} \begin{bmatrix} 0 & 0 & 0 & 0 \\ 0 & 0 & 0 & 0 \\ 1 & 0 & 0 & 0 \\ 0 & 1 & 0 & 0 \end{bmatrix}. \quad (5.16)$$

Thus, the Hamiltonian (5.14) can be written as

$$\begin{aligned} H &= \hbar\omega \begin{bmatrix} 0 & 0 & 0 & 0 \\ 0 & 1 & 0 & 0 \\ 0 & 0 & 0 & 0 \\ 0 & 0 & 0 & 1 \end{bmatrix} + 2\hbar\omega \begin{bmatrix} 0 & 0 & 0 & 0 \\ 0 & 0 & 0 & 0 \\ 0 & 0 & 1 & 0 \\ 0 & 0 & 0 & 1 \end{bmatrix} \\ &= \begin{bmatrix} 0 & 0 & 0 & 0 \\ 0 & \hbar\omega & 0 & 0 \\ 0 & 0 & 2\hbar\omega & 0 \\ 0 & 0 & 0 & 3\hbar\omega \end{bmatrix}, \end{aligned} \quad (5.17)$$

which share the same matrix representation with (5.13). Other boson operators take a more complicated form in the pseudosite representation. Typically, they are represented by a sum over $\sim M$ terms. They can be determined from the definition of the mapping (5.10) and the properties of boson and hard-core boson operators. As an example, we show here how to calculate the representation of b^\dagger which will be frequently used in the following. First we write $b^\dagger = B^\dagger \sqrt{N_b + 1}$, where $B^\dagger |\alpha\rangle = |\alpha + 1\rangle$. The pseudosite operator representation of $\sqrt{N_b + 1}$ is

$$\sqrt{N_b + 1} = \sum_{\alpha=0}^{M-1} \sqrt{\alpha + 1} P_1(r_1) P_2(r_2) \cdots P_N(r_N), \quad (5.18)$$

where $P_j(1) = a_j^\dagger a_j$, $P_j(0) = a_j a_j^\dagger$, and the $r_j (J = 1, \dots, N)$ are given by the mapping (5.10). For B^\dagger we have

$$B^\dagger = a_1^\dagger + a_2^\dagger a_1 + a_3^\dagger a_2 a_1 + \cdots + a_N^\dagger a_{N-1} a_{N-2} \cdots a_1. \quad (5.19)$$

The representation of b^\dagger for any number of pseudosites N is given by the product

of these two operators. For instance, for $N = 2$ pseudosites,

$$\begin{aligned}
\sqrt{N_b + 1} &= \sum_{\alpha=0}^3 \sqrt{\alpha + 1} P_1(r_1) P_2(r_2) \\
&= P_1(0) P_2(0) + \sqrt{2} P_1(1) P_2(0) + \sqrt{3} P_1(0) P_2(1) + 2 P_1(1) P_2(1) \\
&= a_1 a_1^\dagger a_2 a_2^\dagger + \sqrt{2} a_1^\dagger a_1 a_2 a_2^\dagger + \sqrt{3} a_1 a_1^\dagger a_2^\dagger a_2 + 2 a_1^\dagger a_1 a_2^\dagger a_2 \quad (5.20)
\end{aligned}$$

and

$$B^\dagger = a_1^\dagger + a_2^\dagger a_1. \quad (5.21)$$

So

$$b^\dagger = a_1^\dagger + \sqrt{2} a_2^\dagger a_1 + (\sqrt{3} - 1) a_1^\dagger a_2^\dagger a_2. \quad (5.22)$$

where we have applied the commutation relations of pseudosite operators a and a^\dagger . Here, one must be careful because the operators B^\dagger and $\sqrt{N_b + 1}$ do not commute.

The utility of this approach emerges after the transformation to a pseudosites system. Then we have the possibility to apply the density matrix approach to reach a given system by adding pseudosite to pseudosite while truncation is performed. In principle the representation in pseudosites for a given truncated bosonic Hilbert space is an exact transformation. Then we can think in a chain of pseudosites as illustrated in fig. 5.3.

A given pseudosite system can be achieved in the DMRG way by growing up a small system by adding several pseudosite as is illustrated in fig. 5.4.

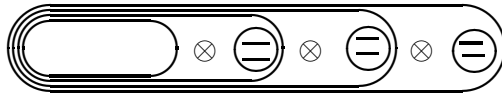


Figure 5.4: *The desired size is reached by adding pseudosites.*

5.5.1 The mapping to pseudosites

Using the transformation to pseudosites we have implemented a density matrix approach to the electron-phonon Hamiltonian (5.1). In this implementation, the

5.5. The pseudosites approach

electron and phonon spaces are treated separately. First, the system is treated as a purely electronic system with a Hamiltonian given by (5.2). We use the basis of two holes in a 3-site system with total spin 0. This electronic space is considered as the initial space over which the pseudosites will be added in the context described above. Then the pseudosites are added to the system and the most important states are used to reduce the Hilbert space. For the phononic part of the Hamiltonian (5.3) basically we use the operators b^\dagger and b . So, initially we need the pseudosite transformations of one of them ¹. First of all, it is important to mention that it must be convenient to add the pseudosite from left to right. This is because in this way we can build up the Hamiltonians as tensor products. So for example, the matrix representation of the operators a and a^\dagger in the $\{|0\rangle, |1\rangle\}$ basis is

$$a = \begin{pmatrix} 0 & 1 \\ 0 & 0 \end{pmatrix} \quad \text{and} \quad a^\dagger = \begin{pmatrix} 0 & 0 \\ 1 & 0 \end{pmatrix}. \quad (5.23)$$

For a two-site system the matrix form of a_1^\dagger and a_2^\dagger must be

$$a_1^\dagger = I \otimes a^\dagger \quad \text{and} \quad a_2^\dagger = a^\dagger \otimes I \quad (5.24)$$

where I is the 2×2 identity matrix (see eqs. (5.15) and (5.16)). The operators a_1 and a_2 must be obtained as the Hermitian of a_1^\dagger and a_2^\dagger respectively. This process is repeated until we have reached 32 Infrared and 32 Raman phonon states in this way forming an exact basis of 9216 states. This means that we have used 10 pseudosites, 5 for the Ir mode and 5 for the Raman one. In general we have found that to find an appropriate configuration for the construction of the entire system is not so easy. Often we have found that performing the pseudosite to pseudosite growing, offset any gain due to the reduction of Hilbert space and is better to make the construction by adding groups of pseudosites. This alternative allow to perform the truncation keeping a low number of important states. Why this occurs is a question not totally understood but may be the answer could be

¹It is important to note that the pseudosite transformation could be used to express exactly the matrix form of a given Hamiltonian.

related to the entanglement of the subsystems with its surrounds in which case we fall in the field of quantum information theory [41]. Another important fact is that exist a dependence between the electron-phonon coupling parameter and the truncation error [23, 41, 42]. This means that with a small value for λ_{I_r}, λ_R (about $0.01eV$) the Hilbert space can be reduced considerably but when these values are increased, the truncation becomes more severe. So we have tested several ways to construct the complete system performing truncation and finally the best way allow us to work with a basis of 288 states, only the 3.125% of the number for the exact Hilbert space basis with a slightly penalty in accuracy (error about 10^{-5}).

5.5.2 Results

To check that no error is done in the calculation of Hilbert space sector, we have calculated exactly the eigenvalues of the electronic Hamiltonian (5.2) for the space sector of one hole, two holes and for the whole Hilbert space. Eigenvalues are plotted in figure (5.5). The basis for the one hole sector consist of the three states $\{| \downarrow, 0, 0 \rangle, |0, \downarrow, 0 \rangle, |0, 0, \downarrow \rangle\}$. Here we can note that the eigenvalues of both sectors coincide with the eigenvalues of the whole Hilbert space as is expected. With this in hand we have calculated the ground state for the electron-phonon system. Figure (5.6) shows a plot of the energy as a function of the number of states kept. The inset shows the same plot for the energy from 128 to 800 states. The black line is the exact ground state energy ($-0.5493118 eV$). Figure (5.7) plots the energies of the ground and first excited states from exact and DMRG calculations with 288 states kept. The ground state is accurately described by DMRG but the first excited state is severely affected.

5.5. The pseudosites approach

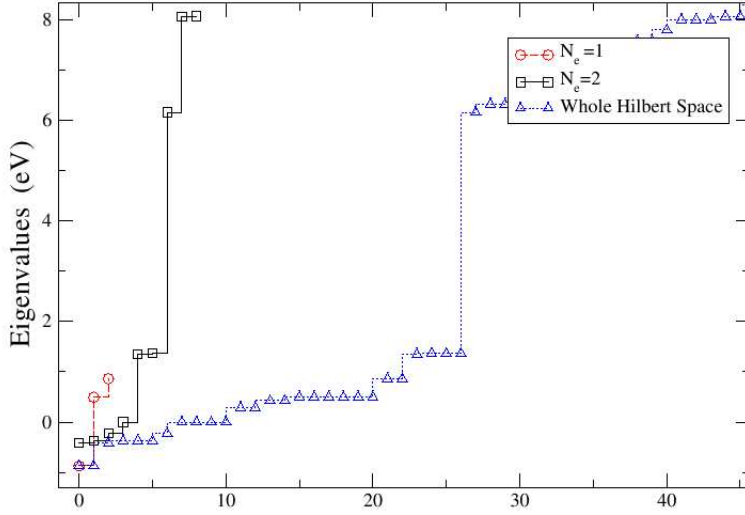


Figure 5.5: *Eigenvalues of the electronic Hamiltonian for one and two holes sectors and whole Hilbert space.*

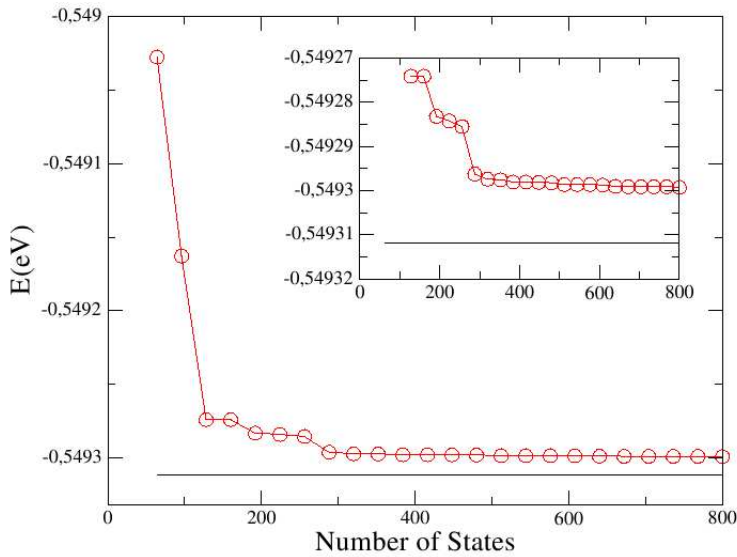


Figure 5.6: *Ground state energy of the electron-phonon system for 32 Raman and 32 IR states with $\lambda_{IR} = \lambda_R = 0.1$ eV as a function of the number of states kept. The inset shows the same plot for $\lambda_{IR} = \lambda_R = 0.01$ eV.*

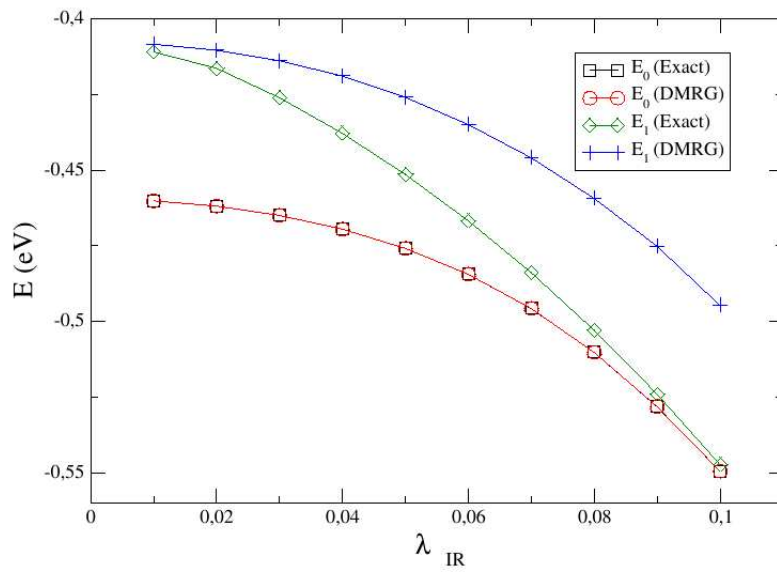


Figure 5.7: λ_R is fixed in 0.1eV. 288 states are kept of a total Hilbert space of 9216 states.

Chapter 6

Conclusions and perspectives

In this thesis we have accurately described the ground state of the one-dimensional Hubbard model with results comparable in accuracy with others in the literature using a finite size DMRG program in which we can make use of the system symmetries.

Furthermore we have worked with an electron-phonon system which have been previously introduced by others authors. For this purpose we have applied two approaches to bosonic systems known as the optimal phonon basis and the pseudosite method. For the first approach, we were not able to compare our results, mainly because the largest size system studied was the 3-site O-Cu-O cluster. The program used in this case is a modification of that used in calculations for the Hubbard model.

With the pseudosite method we have treated the 3-sites cluster with two holes having $S_z = 0$. In this case, due to the relative small Hilbert space size we have been able to calculate exactly the two lower lying eigenstates of the electron-phonon Hamiltonian and compare them to those obtained using the pseudosite method and the density matrix approach.

Despite of the relatively success in the calculations of the ground state for an electron-phonon system, the physical system is not widely discussed and no ground state properties are treated. Here, we have focused on the implementation of the DMRG technique and some related facts.

Another important goal is to improve the computational performance of the DMRG technique. Some improvements would be able to realize in the code optimization and with the wide use of linear algebra packages. Also an object oriented treatment of the algorithms must be exploited.

Calculations on the first excited state must be adapted in the algorithms. This could be useful in calculating the relevant physical information [29].

To treat more than 3 sites within the pseudosite approach is straight forward, so in the future this may also be considered.

Appendix A

The optimal states

Many of the work of White reside in the lectures on statistical mechanics of Feynman [6, 7]. Basically what underscore the method is that in order to know the actual state of a system is sufficient with the information holden in the density matrix. The system of interest is splitted in two parts, one called the *system* and the other the *environment*. The density matrix contains all the information needed from the wavefunction to calculate any property resctricted to the system block. If a operator A acts only on the system block, then

$$\langle A \rangle = \sum_{ii'} A_{ii'} \rho_{ii'} = Tr \rho A. \quad (\text{A.1})$$

Now let us diagonalize the density matrix. Let ρ have eigenstates $|u^\alpha\rangle$ and eigenvalues $\omega_\alpha \geq 0$. Since $Tr \rho = 1$, $\sum_\alpha \omega_\alpha = 1$. Then for any system block operator A ,

$$\langle A \rangle = \sum_\alpha \omega_\alpha \langle u^\alpha | A | u^\alpha \rangle. \quad (\text{A.2})$$

Equation A.2 will apply immediately to our numerical renormalization group procedure. From here we can interpret that w_i is the probability that the system is in the state $|i\rangle$ [6]. If some of these w_i are very low then we do not make a significant error for $\langle A \rangle$ if we ignore them ¹. This idea give rise to the DMRG method and is equivalent to a truncation of the Hilbert space describing the states

¹This is the way to find which states to keep and which to discard [7]

of the system [14]. This argument can be made much more precise. In particular, we can show that keeping the most probable eigenstates of the density matrix gives the most accurate representation of the state of the superblock. Let us assume we have diagonalized the superblock and obtained one particular state $|\psi\rangle$, typically the ground state. We wish to define a procedure for producing a set of states of the system block $|u^\alpha\rangle$, $\alpha = 1, \dots, m$, with $|u^\alpha\rangle = \sum_i u_i^\alpha |i\rangle$, which are optimal for representing ψ . Because we allow only m states, we cannot represent $|\psi\rangle$ exactly if $l > m$, where l is the number of system block states $|i\rangle$. We wish to construct an accurate expansion for $|\psi\rangle$ of the form

$$|\psi\rangle \approx |\bar{\psi}\rangle = \sum_{\alpha,j} a_{\alpha,j} |u^\alpha\rangle |j\rangle. \quad (\text{A.3})$$

In other words, we wish to minimize

$$S = ||\psi\rangle - |\bar{\psi}\rangle|^2 \quad (\text{A.4})$$

by varying over all $a_{\alpha,j}$ and u^α , subject to $\langle u^\alpha | u^{\alpha'} \rangle = \delta_{\alpha\alpha'}$. Without loss of generality, we can write

$$|\bar{\psi}\rangle = \sum_{\alpha} a_{\alpha} |u^\alpha\rangle |v^\alpha\rangle, \quad (\text{A.5})$$

where $v_j^\alpha = \langle j | v^\alpha \rangle = N_{\alpha} a_{\alpha,j}$, with N_{α} chosen to set $\sum_j |v_j^\alpha|^2 = 1$. Switching to matrix notation, we have

$$S = \sum_{ij} (\psi_{ij} - \sum_{\alpha=1}^m a_{\alpha} u_i^{\alpha} v_j^{\alpha})^2, \quad (\text{A.6})$$

and we minimize S over all u^α , v^α , and a_{α} , given the specified value of m . The solution to this minimization problem is known from linear algebra. We now think of ψ_{ij} as a rectangular matrix. The solution is produced by the singular value decomposition of ψ ,

$$\psi = UDV^T, \quad (\text{A.7})$$

where U and D are $l \times l$ matrices, V is an $l \times J$ matrix (where $j = 1, \dots, J$ and we assume $J \geq l$), U is orthogonal, V is column-orthogonal, and the diagonal matrix D contains the singular values of ψ . Linear algebra tells us that the u^α , v^α

Chapter A. The optimal states

and a_α which minimize S are given as follows: the m largest-magnitude diagonal elements of D are the a_α and the corresponding columns of U and V are the u^α and v^α . These optimal states u^α are also eigenvectors of the reduced density matrix of the block as part of the system. This reduced density matrix for the block depends on the state of the system, which in this case is a pure state $|\psi\rangle$. The density matrix, where ψ_{ij} is assumed real, is given by

$$\rho_{ii'} = \sum_j \psi_{ij} \psi_{i'j}. \quad (\text{A.8})$$

We see that

$$\rho = U D^2 U^T \quad (\text{A.9})$$

, i.e. U diagonalizes ρ . The eigenvalues of ρ are $\omega_\alpha = a_\alpha^2$ and the optimal states u^α are the eigenstates of ρ with the largest eigenvalues. Each ω_α represents the probability of the block being in the state u^α , with $\sum_\alpha \omega_\alpha = 1$. The deviation of $P_m = \sum_{\alpha=1}^m \omega_\alpha$ from unity, i.e. the "discarded weight" of the density matrix eigenvalues, measures the accuracy of the truncation to m states. We can say then that if the entire lattice is assumed in a pure state, the optimal states to be kept are the m most important eigenstates of the reduced density matrix of the system block.

BIBLIOGRAPHY

- [1] N. W. Ashcroft and N. D. Mermin, *Solid State Physics*, Brooks Cole (1976).
- [2] F. Mandl, M. A., D. Phil, *Quantum Mechanics* second edition, Butterworths Scientific Publications (1957).
- [3] A. Messiah, *QUANTUM MECHANICS: Two Volumes Bound as One*, Dover Publications, Inc., Mineola, New York (1999).
- [4] C. Cohen-Tannoudji, B. Diu, F. Laloë, *QUANTUM MECHANICS, Vol. I*, Wiley-Interscience (1977).
- [5] E. Kaxiras, *Atomic and Electronic Structure of Solids*, Cambridge University Press (2003).
- [6] R. P. Feynman, *Statistical Mechanics: A set of lectures*, Benjamin, Reading, MA (1972).
- [7] I. Peschel, X. Wang, M. Kaulke and K. Hallberg (Eds.), *Density-Matrix Renormalization: A New Numerical Method in Physics*, Series: Lecture Notes in Physics, Chap. 5 sec. 1 by E. Jeckelmann, C. Zhang and S. R. White, Springer (1998).
- [8] M. W. Long, *The Hubbard Model and some recent applications*
- [9] H. Bruus and K. Flensberg. *Many-Body Quantum Theory in Condensed Matter Physics: An introduction*, Oxford University Press (2004).
- [10] F. H. L. Essler, H. Frahm, F. Göhmann, A. Klümper and V. E. Korepin, *The One-Dimensional Hubbard Model*, Cambridge University Press.

BIBLIOGRAPHY

- [11] H. Tasaki, preprint (1997), cond-mat/9512169.
- [12] H. Tasaki, Prog. Theo. Phys. **99**, 489 (1998).
- [13] S.R. White and R. M. Noack, Phys. Rev. Lett. **68**, 3487 (1992).
- [14] S. R. White, Phys. Rev. Lett. **69**, 2863 (1992).
- [15] S. R. White, Phys. Rev. B **48**, 10345 (1993).
- [16] S. R. White, Phys. Rev. Lett. **77**, 3633 (1996).
- [17] M.A. Martín-Delgado and G. Sierra, Int. Jour. of Mod. Phys. A **11**, 3145 (1996).
- [18] M. A. Martín Delgado, G. Sierra and R. M. Noack. preprint (1999), cond-mat/9903100.
- [19] A. L. Malvezzi, Braz. Jour. of Phys. **33**, 55 (2003).
- [20] E. H. Lieb and F. Y. Wu, Phys. Rev. Lett. **20**, 1445 (1968).
- [21] T. Xiang, preprint (1996), cond-mat/9603020.
- [22] D. Bohr, *The Density Matrix Renormalization Group Applied To Mesoscopic Structures*, M. Sc. Thesis, Thecnical University of Denmark (2004).
- [23] E. Jeckelmann and S. R. White, Phys. Rev. B **57**, 6376 (1998).
- [24] C. Zhang, E. Jeckelmann and S. R. White, Phys. Rev. Lett. **80**, 2661 (1998).
- [25] U. Schollwöck, preprint (2004), cond-mat/0409292
- [26] S. Caprara and A. Rosengren, Nucear Physics B **493** 640 (1997).
- [27] L. Genzel, A. Wittlin, M. Bauer, M. Cardona, E. Schönherr and A. Simon, Phys. Rev. B **40** 2170 (1989).
- [28] I. Batistić, A. R. Bishop, R. L. Martin and Z. Tesanovic, Phys. Rev. B **40**, 6896 (1989).

-
- [29] J. Mustre de Leon, I. Batistić, A. R. Bishop, S. D. Conradson and S. A. Trugman, Phys. Rev. Lett. **68** 3236 (1992).
- [30] J. Mustre de León, S. D. Conradson, I. Batistic and A. R. Bishop, Phys. Rev Lett. **65**, 1675 (1990).
- [31] J. Mustre de León, S. D. Conradson, I. Batistic and A. R. Bishop, Phys. Rev B **44**, 2422 (1991).
- [32] M. I. Salkola, A. R. Bishop, J. Mustre de Leon, and S. A. Trugman, PRB **49**, 3671 (1994).
- [33] M. I. Salkola, A. R. Bishop, S. A. Trugman and J. Mustre de Leon, Phys. Rev. B **51**, 8878 (1995).
- [34] J. Mustre de Leon, R. de Coss, A. R. Bishop and S. A. Trugman, PRB **59**, 8359 (1999).
- [35] J. Miranda-Mena, *Formación Polarónica en Modelos con Interacción Electrón-Fonón. Comparación entre interacción Ionica y Covalente*. M. Sc. Thesis (On the supervision of J. Mustre de León), CINVESTAV Mérida, México (2004).
- [36] J. Miranda-Mena, private communication (2005).
- [37] N. Elstner and H. Monien, preprint (1998), cond-mat/9807033.
- [38] Ramesh W. Pa and Rahul Pandit, preprint (2004), cond-mat/0407011.
- [39] H. Fehske, G. Wellein, G. Hager, A. Weiße, K. W. Becker and A. R. Bishop, preprint (2004) cond-mat/0406023.
- [40] R. J. Bursill, PRB **60**, 1643 (1999).
- [41] R. M. Noack and S. R. Manmana, preprint (2005), cond-mat/0510321.
- [42] G. Hager, E. Jeckelmann, H. Fehske and G. Wellein, Jour. of Comp. Phys. **194**, 795-808 (2004).